Deliverable 5.1
Guidelines on space-*in situ* data assimilation

Deliverable Contributors:	Name	Organisation	Role / Title
Deliverable Leader	Cossarini G.	OGS	WP 5 leader
Contributing Author(s)	Skakala J.	PML	Contributor
	Wakamatsu T.	NERSC	Contributor
	Teruzzi A.	OGS	Contributor
	Spada, S.	OGS	Contributor
	Yumruktepe, C.	NERSC	Contributor
Reviewers	Bertino L.	NERSC	
	Fennel K.	Dalhousie Uni	
Final review and approval	Jozef Skakala	PML	Project Coordinator

Document History:

Release	Date	Reason for Change	Status	Distribution
1.0	28-02-2023	Initial document, reviewed		Internal

To cite this document

Cossarini. *et al.* (2023). D5.1 Guidelines on space-*in situ* data assimilation. Deliverable report of project H2020 SEAMLESS (grant 101004032.). DOI: 10.5281/zenodo.7684591

This project has received funding from the European Union's Horizon 2020 research and innovation programme under grant agreement No 101004032.

TABLE OF CONTENTS

Scope

The scope of this document is (i) to report on the developments and experiments of joint satellite and in situ ensemble biogeochemical data assimilation performed in WP5, and (ii) to provide recommendations to perform joint space-in situ data assimilation in the Marine Copernicus MFC 3D domains.

The partners that support a Copernicus Marine Forecasting Centre (MFC; NERSC for ARC, PML for NWS and OGS for MED) implemented multiplatform (satellite and in situ profile) biogeochemical assimilation experiments in the 1D and 3D setups. This deliverable is built upon deliverables D3.2 (based on 1D experiments) and D3.4 (based on 3D experiments) and the WP4 experiences in setting ensemble 1D and 3D simulations. D5.1 addresses the prospects of joint satellite and profile biogeochemical data assimilation as deemed relevant for each MFC.

Introduction

The assimilation of satellite Ocean Colour observations has been proved to be successful in research and operational applications at both global and regional scales (Fennel et al., 2019; Groom et al., 2019). Chlorophyll concentration is the most commonly assimilated variable (Nerger and Gregg, 2007, 2008; Ciavatta et al., 2016; Fontana et al., 2013; Ford and Barciela, 2017; Gehlen et al., 2015; Hu et al., 2012; Mattern et al., 2017; Teruzzi et al., 2018; Tsiaras et al., 2017, Pradhan et al., 2019), but other remote sensing variables have also been tested: diffuse attenuation coefficient, phytoplankton functional types, particulate organic carbon and inherent optical properties (Ciavatta et al., 2019, 2018, 2014; Jones et al., 2016; Shulman et al., 2013; Skákala et al., 2018; Xiao and Friedrichs, 2014, Pradhan et al. 2020).

Ocean colour has the unique capability to provide frequent, global-scale observations of the biological components of the surface of the ocean but the propagation of surface information towards deeper marine layers requires approximations. For instance, in variational assimilation the vertical covariance can be parameterized by synthetic vertical profiles obtained by previous model simulations (Teruzzi et al., 2018) while EnKF-like assimilation schemes may have limitations in deeper ocean layer (Fontana et al., 2013; Hu et al., 2012, Simon et al. 2015) and require localization in the vertical direction to tackle spurious correlations (Goodliff et al., 2019; Pradhan et al., 2019).

On the other hand, in situ observations bring information on processes occurring in the ocean interior (e.g., deep chlorophyll maximum, vertical fluxes of nutrients and organic matter). In situ data from traditional fixed monitoring stations are invaluable in providing information on the long-term trends of the ocean ecosystems (e.g., Widdicombe et al., 2010). Additionally, operational autonomous sensors, such as BGC-Argo floats or BGC-gliders, provide frequent and high-resolution water column descriptions for open sea and coastal areas (Bittig et al., 2019; Testor et al., 2019). Despite their importance, there are only few examples of assimilation of in situ biogeochemical profiles. Cossarini et al. (2019) and Verdy and Mazloff (2017) assimilated BGC-Argo floats improving vertical variability of biogeochemical processes (e.g., the depth of the deep chlorophyll maximum). Kaufman et al. (2018) showed that the assimilation of BGC data from gliders is effective to constrain depth-integrated primary production and carbon export. In Liu et al. (2017), in situ BGC data from fixed stations is assimilated to provide nutrient-transport estimations in a thirty-year reanalysis of the Baltic Sea.

The integrated assimilation of biogeochemical observations from satellites and in situ profile platforms is in its infancy (Skakala et al., 2020, Teruzzi et al., 2021, Yu et al., 2018, Ford et al., 2021) and surface ocean colour observations remain largely the only data assimilated in the contest of biogeochemical operational systems (Le Traon et al., 2019).

The overall objectives of WP5 are (i) to enable biogeochemical model systems to assimilate biogeochemical observations from the Copernicus space element and in situ platforms consistently, and (ii) to link better the surface and subsurface ecosystem dynamics to improve the predictions of water quality, carbon cycle and food web indicators.
Our hypotheses are the following:

- new ensemble data assimilation methods can better estimate model covariances linking surface to subsurface processes;
- the integration of the satellite observations and in situ ocean data can increase the controllability of biogeochemical states and processes along the water column.

This document is structured as follow: section 3 describes the choices for the experiment designs used in the different MFC domains. The results of the assimilation experiments obtained in the 1D (Task 5.1) and 3D (Task 5.2) configurations of the different MFC model systems are reported in section 4. Ensemble diagnostics are described in terms of (i) observed state variables, (ii) non-observed state variables, and (iii) relevant SEAMLESS indicators (leveraging from the conclusions of Tasks 3.2 and 3.3). In section 5, the results obtained for indicators (phenology, POC flux, primary production, grazing efficiency, PFTs, Ph and O2) are discussed. Finally in section 6, we outline and discuss the guidelines for the implementation of multiplatform data assimilation in the other Copernicus MFCs.

Experimental Design Choices

In this section, the choices for the assimilation experiments are described. This builds on the assimilation methods developed and tested by the partners in WP2 and WP3 where the ensemble data assimilation methods have been developed and implemented in the 1D SEAMLESS prototype and in the 3D MFC model systems. In the present deliverable, the focus is to assess (i) the options for ensemble generation that optimize the covariances description linking adequately surface and subsurface dynamics and (ii) the configuration for the multiplatform data assimilation.
In particular, the ensemble generation in the 1D systems includes the random atmospheric forcing, initial conditions, and the uncertainty of biogeochemical model parameters. On the other hand, adjustable aspects of the multiplatform data assimilation are:

- impact of the assimilation of in situ profile observations beside Ocean Color data;
- frequency of the assimilation for Ocean Color observations;
- different values for the observation errors for ocean colour and profiles of the same variable;
- vertical spatial resolution of profile observations;
- forgetting factor (inflation).

The 3D MFC systems are much more computationally expensive than the 1D SEAMLESS prototype. Thus, the 1D system experiments are beneficial for the limited testing possibility of different configurations in the 3D MFC systems.
A schematic illustration of the ensemble-based assimilation methods and setup of 1D and 3D systems is given in Table 3.1. Details of the different system are then provided in the following sections.

Partner	CMEMS MFC	Assimilated variables			Ensemble data assimilation methods in 1D and 3D systems	investigated options
		Remote sensing data	Profiles in 1D experiments	Profiles in 3D experiments		

NERSC	**ARC**	Chlorophyll from CMEMS OC TAC	Chlorophyll from BGC-Argo	Chlorophyll from BGC-Argo and nutrient profiles from CMEMS INSITU TAC	EnKF	Ensemble generation, frequency of OC DA, observation errors
PML	**NWS**	PFT chlorophyll from CMEMS OC TAC	Temp, chlorophyll, oxygen from L4 and semi-synthetic profiles	Temp., Sal, Chlorophyll, oxygen, from EN4 (Hadley data-set) + glider	Ensemble-3DVAR	Ensemble generation, frequency of OC DA, depth of observations, observation errors
OGS	**MED**	Chlorophyll from CMEMS OC TAC	Chlorophyll from BGC-Argo	Chlorophyll from BGC-Argo	SEIK	Ensemble generation, frequency of OC DA, observation errors

Table 3.1: Overview of model configurations, observations and data assimilation methods used in this report.

3.1 Experimental design for the MED model system

3.1.1 MED 1D model system

GOTM-FABM-BFM 1D model.

The Task 5.1 aims at investigating various aspects of multi-platform assimilation in the 1D prototype of FABM-BFM implemented in WP2. In particular, the SEAMLESS 1D-prototype system has been applied using BGC-Argo and satellite data in two Mediterranean Sea locations in 2019 (one in the west and one in the east; orange boxes in Fig. 3.1.1) following the testing framework adopted in WP4.

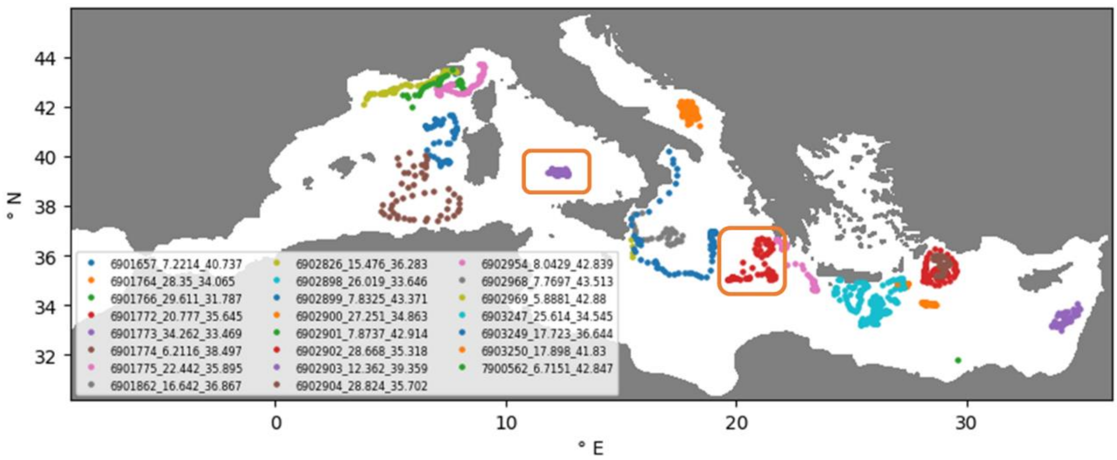

Figure 3.1.1: Location of 2019 BGC-Argo floats equipped with nitrate sensors. Floats in the orange rectangles have been used in the 1D assimilative experiments: 6902903 and 6901772 BGC-Argo floats in the Tyrrhenian Sea (western Med) and in the Levantine (eastern Med), respectively.

Observations

Chlorophyll concentration from the two selected BGC-Argo (wmo: 6902903 and 6901772) and from satellite observations were used for assimilation in the 1D prototype. Satellite chlorophyll concentration are the multi-sensor ocean colour product from Copernicus Marine Services (i.e., OCEANCOLOUR_MED_BGC_L3_NRT_009_141/ in https://data.marine.copernicus.eu), while BGC-Argo chlorophyll are from the Coriolis repository (https://www.coriolis.eu.org/Data-Products/Data-Delivery). The observation errors are composed of a multiplicative and an additive part. The additive error has been kept constant and equal to 0.02 mg/m3 while different values were tested for the multiplicative one. All the assimilated state variables are log-transformed.

The EAT data assimilation system and ensemble setup

Using the EAT framework several experiments using the ESTKF have been carried out at the two float locations: 6902903 and 6901772 (Figure 3.1.1). The ESTKF is one of the ensemble assimilation methods available in EAT, and it provides analogous results to the version of the SEIK filter implemented in the 3D system. As discussed in Nerger et al (2012), the two filters are equivalent in case of random ensemble transformation.
The ensemble had 50 members and it was generated through:

- different initial conditions obtained by an ensemble spin-up simulation using different meteorological forcing;
- different sets of BFM parameters, where the nine most relevant parameters identified in WP3 were randomly perturbed using a uniform distribution with +/-20% range. Each set of perturbed parameters were kept constant along the one-year simulations.

List of 1D experiments and options tested for multiplatform data assimilation

A number of assimilation settings were tested using the 1D SEAMLESS prototype (Table 3.1.1): the observation types, the frequency of the satellite observations assimilation, the observation errors of satellite and floats data.

Run name	Chlorophyll: types of observations	Assimilation frequency	Observation error (multiplicative component)
ENS	-	-	-
ESTKF satw_low	Satellite	weekly	20%
ESTKF satd_low	Satellite	daily	20%
ESTKF satd_high	Satellite	daily	35%
ESTKF float_low	Float	daily	20%
ESTKF satw_low+float_high	Satellite Float	weekly daily	20% 35%
ESTKF satd_high+float_low	Satellite Float	daily daily	35% 20%

Table 3.1.1: list of 1D experiment and options tested with the 1D SEAMLESS prototype.

3.1.2 MED 3D MFC domain

3D OGSTM-BFM

OGSTM–BFM is the model in use for biogeochemistry in the MED MFC (Salon et al., 2019) forced offline by ocean dynamics provided by NEMO-OceanVar. OGSTM solves the transport of tracers. BFM solves the biogeochemical evolution of 51 prognostic variables of the low trophic level (see the SEAMLESS deliverable D2.2 and reference cited therein).

Observations

Observations are the same described for the 1D framework: ocean colour from L3 Copernicus OC TAC and chlorophyll profiles from BGC-Argo float from Coriolis GDAC. The only difference is that, in the 3D framework all the BGC-Argo floats (23 of them) mounted with chlorophyll sensors in 2019 were assimilated (Fig. 3.1.1.1)

The data assimilation system and ensemble setup

The 3D assimilation experiments are conducted using the SEIK-OGSTM system developed in SEAMLESS and described in WP3.4. In order to achieve multiplatform assimilation, the system has been improved to support both satellite and BGC-Argo float profile observations.
SEIK-OGSTM log-transforms concentrations of both model and observations, and avoids spurious covariances below the euphotic layer by applying a threshold on low concentrations before the assimilation. Ensemble consists of 24 members, and each ensemble member starts from a different IC and uses a different set of BFM parameters.
Inflation and localization techniques are also applied at each assimilation.

List of 3D experiments and options tested for multiplatform data assimilation

Assimilation experiments focus on two relevant periods: (i) winter surface bloom dynamics (February–March 2019) and (ii) summer stratification and Deep Chlorophyll Maximum dynamics (July-August 2019). Ensemble size (24 ensemble members) and ICs generation method are those used in WP3.4, while the perturbed BFM parameters are the full set of 9-parameters selected in the sensitivity of WP2.3. Parameters perturbation draws from a uniform distribution within an interval of +/- 20%. In addition to parameters perturbation, the ensemble spread has been preserved using a forgetting factor of 0.9.
The error of observations also counts two components: an additive and a multiplicative ones. In accordance with the 1D results, the additive error has been set to 0.02 mg/m^3, while some tests were performed to assess the effect of using different multiplicative error in satellite and floats (Tab. 3.1.2). In order to avoid spurious correlation, localization (with a horizontal radius of nearly 125 km) and low concentrations cut-off (threshold: 1.e-5) were applied as in WP3.4 experiments. Additionally, standard deviations of the ensemble are checked before each assimilation step and rescaled wherever they are higher than 1 in the log-transformed space.

Run name	Simulated period	Type of assimilated chlorophyll observations	Observation error (multiplicative component)
ENS	Winter and summer	-	-
SEIK OC	Winter and summer	Satellite	30%
SEIK OC ARGO	Winter	Satellite Float	30%
SEIK OC ARGOlow	Winter and summer	Satellite Float	30% 20%

Table 3.1.2: list of 3D experiment and options tested in the Mediterranean Sea MFC domain.

3.2 Experimental design for the ARC model system

3.2.1 ARC 1D model system

GOTM-FABM-ECOSMO 1D model.

Under Task 5.1, various aspects of multi-platform assimilation were investigated in the ARC domain with the SEAMLESS 1D prototype system GOTM-FABM-ECOSMO as implemented in WP4. The SEAMLESS 1D-prototype system is used for testing the impact of BGC-Argo and satellite data in the southern basin of the Norwegian Sea in 2020 following the experimental framework established in WP4 (1D data assimilation experiments).

Observations.

Chlorophyll-a concentration profile data from BGC-Argo (wmo id: 6903554, see figure 3.2.1.a) and surface Chlorophyll-a data from ESA OC-CCI satellite ocean color data Ver4.2 (Sathyendranath et al 2020) were used for assimilation in the 1D prototype. Satellite estimates of chlorophyll concentration are obtained from the ESA ocean color project (http://www.oceancolour.org) and BGC-Argo chlorophyll-a data are obtained from the Coriolis repository, both are also available from the CMEMS server. The observation errors are assumed to be additive and the standard deviation of the error is set to be proportional to the absolute value of the observation value, following the log-normal probability distribution. Both observations are log-transformed first and the additive error is defined based on the transformed value. The amplitudes of standard error are set to 20% for the Argo float data and 30% for the satellite ocean color data, respectively. Both Argo float data and satellite data are linearly interpolated to sampling time stamps with 8-day and 5-day sampling intervals along the Argo trajectory.

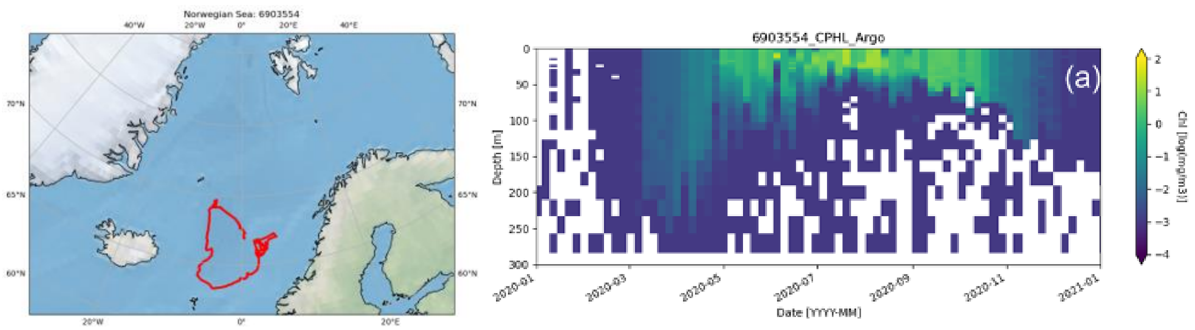

Figure 3.2.1 Trajectory of Argo float 6903554 (left panel) in the Norwegian Sea and vertical profile of chlorophyll-a (right panel) in 2020.

The EAT data assimilation system and ensemble setup

Following a spinup run of a GOTM single run from 2011 to 2019 initialized with climatological temperature/salinity and BGC variables, an initial model ensemble is generated by the GOTM ensemble runs from 2019 January 1st to 2020 April 6th. The sources of model uncertainty are given by 20% of perturbations in the two components of 10-m wind and downward shortwave radiation along the Argo trajectory and 20% of perturbations in the ECOSMO model parameters. The data assimilation scheme is the EnKF with log transformation of selected state variables consisting of two phytoplankton biomass (diatom and flagellate), two zooplankton biomass (large and small zooplankton), two phytoplankton/chlorophyll concentrations (diatom and flagellate) and three nutrients (nitrate, phosphate, silicate). The ensemble size is 80 members. The period of the assimilation experiments is from March 2020 to August 2020.

List of 1D experiments and options tested for multiplatform data assimilation

Four experiments, EX1, EX2, EX3 and EX4 were conducted to investigate the impact of different settings of multiplatform observation regarding combinations of two observational platforms, satellite and Argo float, and combinations of sampling frequencies, 8 days and 5 days intervals.

Run name	Types of observation	Analysis Frequency	Observation Error [%]
EX1	Satellite Chl-a concentration Argo Chl-a concentration	8 days 8 days	30% 20%
EX2	Satellite Chl-a concentration	8 days	30%
EX3	Satellite Chl-a concentration Argo Chl-a concentration	5 days 5 days	30% 20%
EX4	Satellite Chl-a concentration	5 days	30%

Table 3.2.1 list of data assimilation experiments and options in the SEAMLESS 1D prototype setup in the Norwegian Sea.

3.2.2 ARC 3D MFC domain

3D HYCOM-FABM-ECOSMO.

The Biogeochemical (BGC) reanalysis system was developed based on the HYCOM-ECOSMO II ocean-ice-biogeochemical coupled model. The ocean model is based on HYCOM 2.2.37, coupled to a sea ice model. The vertical coordinate is isopycnal in the stratified open ocean and z-coordinates in the unstratified surface mixed layer. The model domain covers the North Atlantic and Arctic basins, with 216*144 horizontal grid points, with approximately 50 km grid spacing and 28 hybrid vertical layers. The top five target densities are purposely low to force them to remain z-coordinates. The minimum z-level thickness of the top layer is 3 m. ECOSMO II contains 14 prognostic BGC variables: nitrate, ammonium, phosphate, silicate, diatoms, flagellates, micro- and meso-zooplankton, particular and dissolved organic matter, opal, oxygen and chlorophyll concentrations associated with the two phytoplankton groups.

Observations

The sources of satellite and BGC Argo chlorophyll data are the same as described in the 1D setup (section 3.2.1). Argo profile data are interpolated to ESA OC-CCI v4.2 8-daily product time stamps so that both data sampling frequencies matche. Further, both satellite and Argo data are thinned by averaging profiles collected within a given model grid cell (superobing). Seven BGC Argo floats are available in the Norwegian Sea domain in 2019 (see Figure 3.2.2) and 2-3 Argo profiles are assimilated per assimilation cycle. The observation errors of the assimilated data are the same as in the 1D setting (see table 3.2.2).

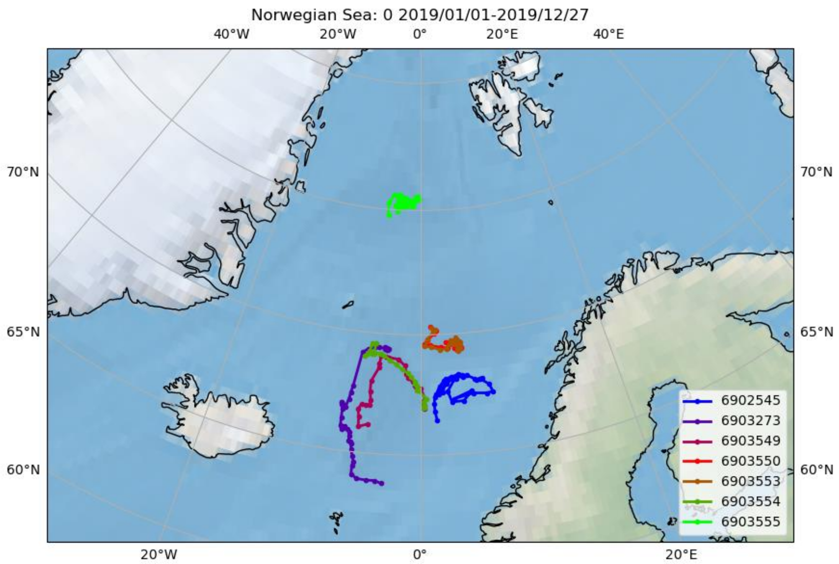

Figure 3.2.2 Trajectory and sampling points of Argo floats (wmo id: 6902545, 6903273, 6903549, 6903550, 6903553, 6903554, 6903555) in the Norwegian Sea in 2019.

The data assimilation system and ensemble setup

The ARC 3D MFC system is joint state-parameter estimation system with the ensemble Kalman filter and smoother for the ECOSMO biogeochemical state and parameters. The operational ARC MFC system was updated for Argo float data assimilation under SEAMLESS WP5. The joint state-parameter estimation is based on the TOPAZ Deterministic Ensemble Kalman filter system (DEnKF) used in a one-lag smoother (EnKS) setting. Localization radius of local analysis is set to 200km uniform over the model domain. The model is HYCOM-EVP-ECOSMO, coupled online. A log- transformation is applied to the biogeochemical variables Chl-a, nitrate, silicate and phosphate and a bounded beta distribution is applied to the model parameters. Assimilation masks are defined by sea-ice concentration, mixed layer depth and surface nitrate concentration criterions in order to mitigate analysis instability related to a model bias in the timing of phytoplankton phenology. Only biogeochemical data are assimilated (surface chlorophyll concentration from satellite ocean colour, chlorophyll concentration profiles from BGC-Argo floats) and updated by data assimilation. The assimilation cycles are defined by the frequency of the composite satellite ocean colour data ESA OC-CCI v4.2 8-daily product. The period of data assimilation experiments is set from to March 2019 to August 2019. The ensemble generation is the same as described for the 1D setting, except that the random model forcing is spatially autocorrelated with a 250 km scale using a spectral method.

List of 3D experiments and options tested for multiplatform data assimilation

Three experiments, EX0, EX1 and EX2 were conducted to investigate the impact of different settings of multiplatform observation regarding combination of two observational platforms, satellite and Argo float.

Run name	Types of observation	Analysis Frequency	Observation Error [%]
EX0 (model free run)	No observation	N/A	N/A
EX1 (w/o Argo)	Satellite Chl-a concentration	8 days	30%

EX2 (w/ Argo)	Satellite Chl-a concentration Argo Chl-a concentration	8 days 8 days	30% 20%

Table 3.2.2 list of data assimilation experiments and options in the ARC 3D MFC.

3.3 Experimental design for the NWS model system

3.3.1 NWS 1D model system

GOTM-FABM-ERSEM 1D model.

We used the set-up developed and tested in WP2 and WP3 as described in D3.2: the 1D configuration is based at the L4 station in the Western English Channel. The L4 location is 50m deep, lies about 12km far from the Plymouth Sound and is seasonally stratified. The L4 1D model set-up has 100 vertical layers, and uses atmospheric forcing extracted from the ERA5 product. The model was spun up starting from 01/01/2007 and prepared for a set of 1-year simulations for the period between 01/11/2014 and 31/10/2015.

Observations.

To perform the desired experiments, we found it optimal to use "semi-synthetic" observations provided by a bi-decadal (23 year) reanalysis data assimilating phytoplankton functional types (PFT) surface chlorophyll from ocean colour – climate change initiative (OC-CCI), satellite sea surface temperature (SST), as well as temperature and salinity from the Met Office Hadley centre EN4 data-set. The advantage of the reanalysis is that it is nearly identical to the assimilated observations near the observation locations (e.g. Skakala et al. 2018, 2020, 2021, 2022), whilst it naturally extrapolates the observations into locations with observational gaps. The complete data set provided by the re-analysis (no data gaps) is ideal for the experiments in this study, where data with different sampling frequency are assimilated and compared. The reanalysis data were complemented by the L4 observations (from the surface, or very near the surface) for temperature, chlorophyll and oxygen. The L4 data sampling frequency was 5 days. None of the reanalysis/observation data had uncertainties provided, so all the uncertainties in the 1D experiments were set to be 10% from the observed value.

The EAT data assimilation system and ensemble setup

We have run simulations with 30 member ensembles using the EAT software, i.e. by perturbing the initial value conditions, atmospheric forcing (re-scaling the forcing data by 10%) and using the perturbations of the selected 6 most sensitive ERSEM parameters (based on the analysis from WP3.2 and applied in 3D within WP3 and WP4). The ERSEM parameters were, similarly to the 3D case, drawn from a uniform distribution within an interval of +/- 30% around the established parameter value (from Butenschön et al, 2016). The DA was based on ensemble-3DVAR filter from the PDAF implementation within EAT.

List of 1D experiments and options tested for multiplatform data assimilation

The 1D 30-member ensemble experiments that we performed at L4 location are summarized in Tab.3.3.1. The options tested are: the observation types, the assimilation frequency of the satellite observations, space frequency of observations, the observation errors.

Run name	Types of assimilated observations	Assimilation frequency	Depths of observations	Observation error
Free run	-	-	-	
SST-1day	Reanalysis SST	1 day	surface	10%
SST-5day	Reanalysis SST	5 day	surface	10%
SST-10day	Reanalysis SST	10 day	surface	10%
CHL-1day	Reanalysis surface chlorophyll	1 day	surface	10%
CHL-5day	Reanalysis surface chlorophyll	5 day	surface	10%
CHL-10day	Reanalysis surface chlorophyll	10 day	surface	10%
T-3depths	Reanalysis temperature	1 day	3 depths at 0, 25, 50 m	10%
T-6depths	Reanalysis temperature	1 day	6 depths, each 10m	10%
T-51depths	Reanalysis temperature	1 day	51 depths, each 1 m	10%
CHL-3depths	Reanalysis chlorophyll	1 day	3 depths at 0, 25, 50 m	10%
CHL-6depths	Reanalysis chlorophyll	1 day	6 depths, each 10m	10%
CHL-51depths	Reanalysis chlorophyll	1 day	51 depths, each 1 m	10%
Multi-DA	Reanalysis SST, surface chlorophyll, L4 temperature, chlorophyll, oxygen	1 day	wherever available	10%

Table 3.3.1: Description of the simulations tested in the 1D case.

3.3.2 NWS 3D MFC domain

3D NEMO-ERSEM

The NEMO-FABM-ERSEM configuration used in this study was the same than in all the previous experiments of WP3 and WP4 (e.g. described in D3.4, D4.1, D4.2).

Observations.

The multiplatform DA was assimilating all the observations as the weakly and strongly coupled runs in D4.1 and D4.2 (satellite SST, EN4 temperature and salinity, and OC surface chlorophyll) together with chlorophyll and oxygen from gliders, that operated in the central North Sea (see Fig.3.3.1). The gliders were delivered by the UK AlterEco programme and provided data from the late 2017 to the early 2019.

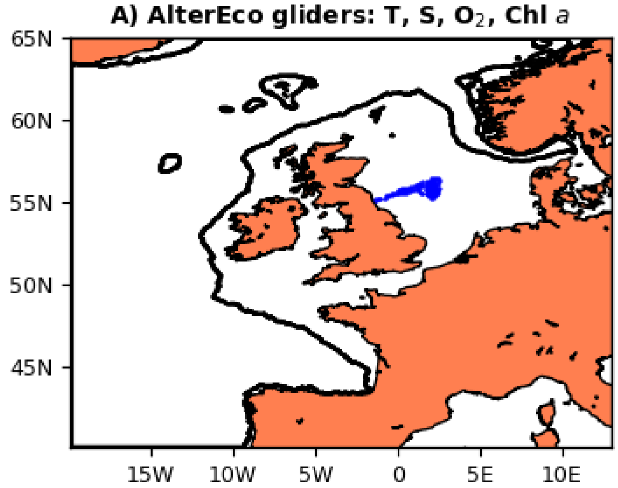

Figure 3.3.1 The locations of AlterEco gliders during the 2018 mission that were assimilated into the model within the multi-platform DA.

The data assimilation system and ensemble setup

We used the weakly coupled ensemble-3DVAR (NEMOVAR) system developed in WP3 and WP4 and described in D3.4 and D4.1. To summarize: the system uses a 30-member ensemble based on 10-member ensemble of ERA5 atmospheric forcing, observation perturbations and perturbations of the 6 most sensitive ERSEM parameters from the WP3.2 analysis. All the available data are assimilated on a daily basis and the system uses the FGAT approach (First Guess at Appropriate Time). The physical DA updates temperature, salinity, sea surface height (SSH) and horizontal velocity components through a set of balancing linear transformations, whilst biogeochemical DA is always univariate, with a balancing module used to spread increments from the observed variables into the unobserved variables (e.g., Skakala et al (2020,2021)). In its most typical case, total chlorophyll increments are spread into phytoplankton function type (PFT) chlorophyll increments and subsequently to all the other PFT biomass components by using background community structure and stoichiometry.

List of 3D experiments and options tested for multiplatform data assimilation

Two simulations were compared in this study, (i) the weakly coupled ensemble-3DVar run from D4.1 assimilating SST, surface chlorophyll and EN4 temperature and salinity, with (ii) the multi-platform DA run assimilating on top of that also glider chlorophyll, temperature and oxygen. The simulations were run for the January – June 2018 period.

Results of assimilation experiments

This section reports the results of the assimilation experiments of the different 1D model systems (task WP5.1) and of the 3D MFCs model (task WP5.2). Results are reported in terms of diagnostics for observed and non-observed variables, and for the SEAMLESS ecosystem indicators.

4.1 Assimilation results in the MED MFC domain

Diagnostics on observed and non-observed variables in 1D system

The impact of multiplatform (i.e., satellite and BGC-Argo chlorophyll observations) assimilation is shown in the chlorophyll Hovmöller diagrams of Figure 4.1.1 for the two selected locations: the BGC-Argo 6902903 in the western Mediterranean Sea (left column) and 6901772 in the eastern Mediterranean Sea (right column). The two locations represent two different bioregions and trophic regimes in the Mediterranean Sea: less oligotrophic, and more intense and lasting surface winter bloom in the west and deeper deep chlorophyll maximum (DCM) dynamics in the eastern location. The assimilation of satellite chlorophyll observations impact both the winter bloom (changes in intensity and timing of the bloom) and the DCM dynamics in summer (mainly changes in the vertical displacement of the DCM; rows 2, 3 and 4 of Fig. 4.1.1). Among the three satellite-only assimilation runs, the most intense changes (positive and negative patches in the Hovmöller diagram of rows 2, 3 and 4 in Fig. 4.1.1) are provided by the one with the highest assimilation frequency (i.e., satd with respect to satw) and the one with the lowest satellite error (i.e., satd_low with respect to satd_high). The addition of the assimilation of BGC-Argo float observations introduces new features with respect to the satellite-only assimilation (rows 6, and 7 of Fig. 4.1.1). In particular, some small new features are visible during the winter surface bloom (see for example the differences between ESTKF satd_high+float_low – sixth row - and ESTKF satd_high - third row- in the western location). Then, the timing of the onset of DCM and the DCM dynamics during summer are further changed by BGC-Argo assimilation (see for example the eastern location, right column in Fig. 4.1.1). Additionally, the chlorophyll profile assimilation can change the sign of the correction with respect to those of the satellite-only assimilation (e.g., satd_high+float_low in the west in Fig. 4.1.1). Finally, the comparison of the runs shows that the lower the BGC-Argo error (i.e., float_low), the higher the impact of BGC-Argo with respect to the impact of satellite data.
The assessment of the assimilative experiments on the observed variable (i.e., chlorophyll) is performed computing the RMSD of simulations against satellite data for the four seasons (Fig. 4.1.2) and the RMSD of simulations against profiles for selected vertical layers (0-50m 50-100m and 100-150m) on a daily basis (Fig. 4.1.3). These skill performance statistics are computed on model-observation misfit before the assimilation. In general, the assimilation of satellite observations improves, as expected, the statistics computed on satellite data with the best performance obtained by the run with daily satellite assimilation and lower observation error. The assimilation of vertical chlorophyll profiles-only improves significantly the statistics based on BGC-Argo floats in the western location during spring, summer and autumn (Fig. 4.1.2). On the other hand, a too small variance of the ensemble prevents the assimilation to correct the large winter bias at surface. In the eastern location, the float assimilation impacts the timing of the onset of the deep chlorophyll maximum (Fig. 4.1.1). However, statistics averaged over the selected layers and seasons do not clearly capture this improvement (Fig. 4.1.3) and some degradations are, instead, observed.
Considering the jointly OC and profile assimilation, it must be noted the presence of inconsistencies between the satellite and BGC-Argo observations at surface (first row in Fig. 4.1.1), which were already noticed for the Mediterranean Sea (Teruzzi et al., 2021), that might introduce contrasting effects between the assimilation of the two observation types. However, the multiplatform assimilation (e.g., satd_high+float_low) has skill performance almost equal to the one of the satd_low assimilation for OC data, and equal and even better than the ones of the float_low assimilation for BGC-Argo data. We can conclude that the multiplatform ensemble data assimilation can efficiently handle the potential inconsistencies between different observation types.

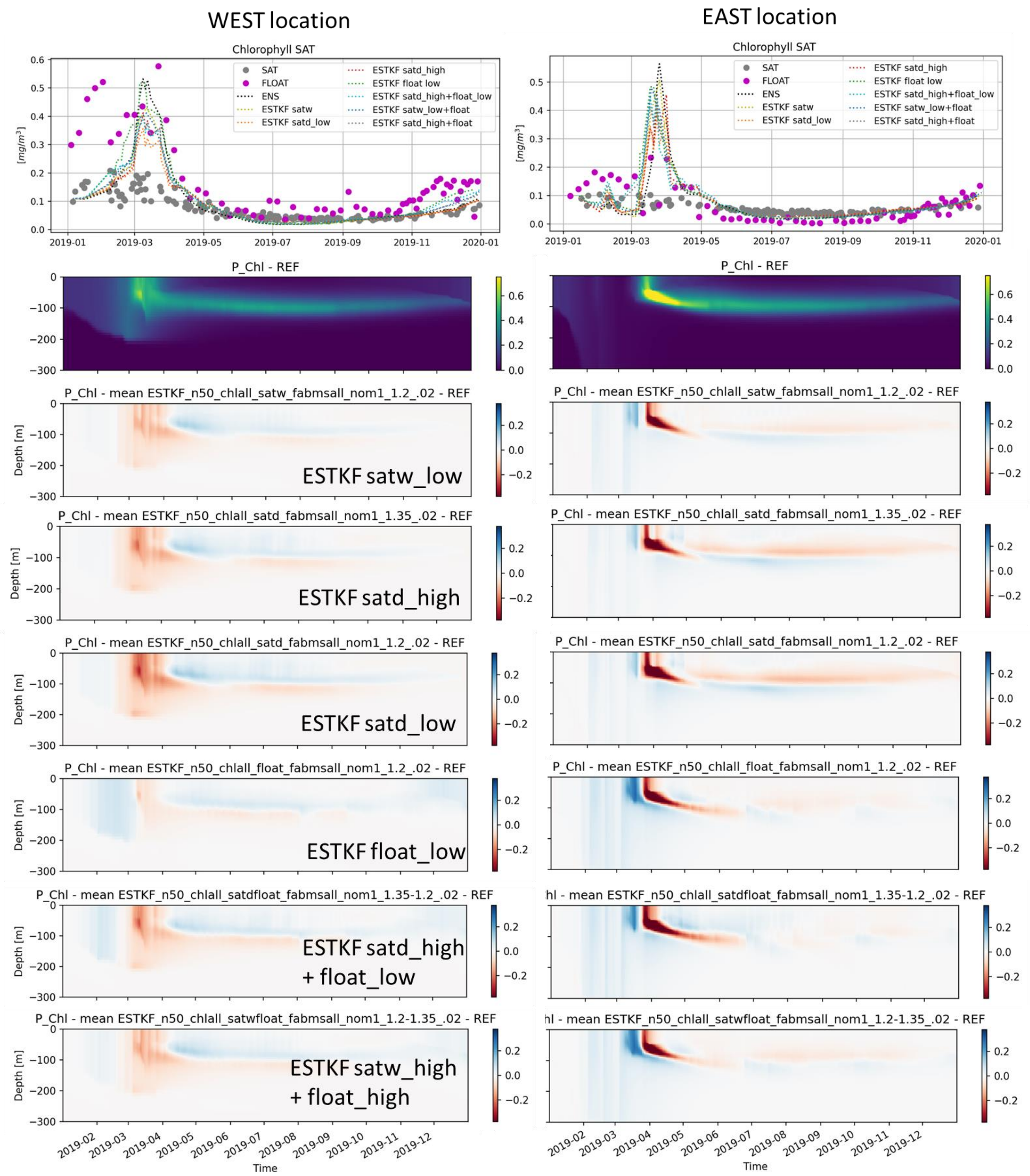

Figure 4.1.1: Hovmöller diagrams of chlorophyll [mg CHL m-3] of the reference run (first row) and the difference between assimilative runs and the reference (from 2nd to 6th rows) for the western and the eastern locations.

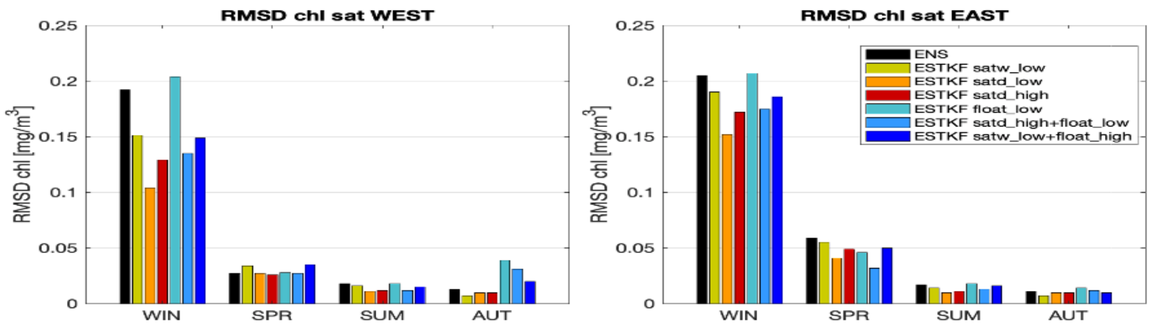

Figure 4.1.2: chlorophyll RMSD with respect to satellite surface data for the WEST (left) and EAST (right) Mediterranean location runs.

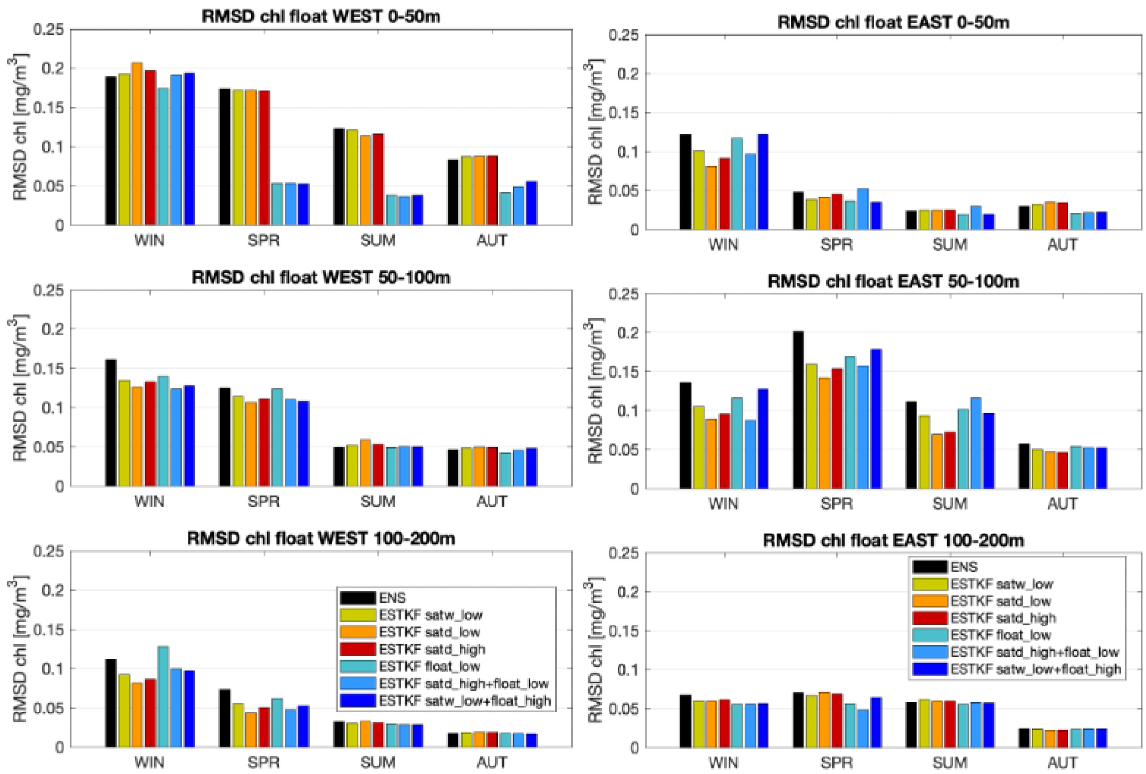

Figure 4.1.3: Chlorophyll RMSD with respect to BGC-Argo float data for selected vertical layers (0-50m: first row; 50-100m: second row; 100-200m third row) for the WEST (left column) and EAST (right column) Mediterranean location runs.

The availability of nitrate from BGC-Argo (a non-observed variable) allows to assess how the different types of chlorophyll observations impact other model components. Figure 4.1.4 shows the nitrate RMSD computed for selected seasons and layers (0-50m, 50-100m, 100-200m, 200-400m). The two locations exhibit different performance behaviors, with a general improvement of RMSD values in the eastern Mediterranean location but a degrading RMSDs in the western Mediterranean. The best performances are generally obtained with the satellite-only assimilation: assimilating chlorophyll profiles does not have always a positive impact on the quality of nitrate. In some cases, lower performances for nitrate metrics occur correspondently to lower chlorophyll performances (e.g., at 0-50m in spring and summer for satd_high+float_low, at 100-200m in spring for satw_low+float_high) suggesting that a degradation in nitrate (and possibly on other nutrients) could affect phytoplankton dynamics contrasting the benefit of float chlorophyll assimilation. Degradation of other biogeochemical variables after chlorophyll-only profiles assimilation is shown in Wang et al., (2020). Further investigations are needed to fully understand the impact of ensemble data assimilation methods in shaping multivariate covariances in a contest of multiplatform assimilation and several aspects should be considered.

Simulations could be performed for all BGC-Argo floats with chlorophyll, nitrate and bbp700 (e.g., phytoplankton biomass) measurements to get more statically robust results when chlorophyll-only is assimilated. On the other hand, it must be noted that joint assimilation of multiple biogeochemical variables (Wang et al., 2020, Teruzzi et al., 2021) can provide better constrain to biogeochemical dynamics proven the availability of multivariate data from the same BGC-Argo float locations.

Indeed, nitrate is not the limiting nutrient in the Mediterranean Sea (Lazzari et al., 2016). Thus, covariance between chlorophyll and nitrate reflects the actual relationship between the two variables at the time of assimilation but not the relationship between the limiting nutrient (e.g., phosphate) and chlorophyll that drove the observed values of chlorophyll at the time of the assimilation. Thus, the assimilation framework would better work if nutrients were also assimilated (see for example Teruzzi et al., 2021) or if assimilation smoothers were used instead of filters, and phosphate observations (whether available) should be used. Additionally, as shown in Wang et al. (2020), jointly chlorophyll and backscatter (bbp700) profiles better constrain phytoplankton biomass and the dynamically varying chlorophyll to carbon ratio with benefits for simulated biogeochemical dynamics.

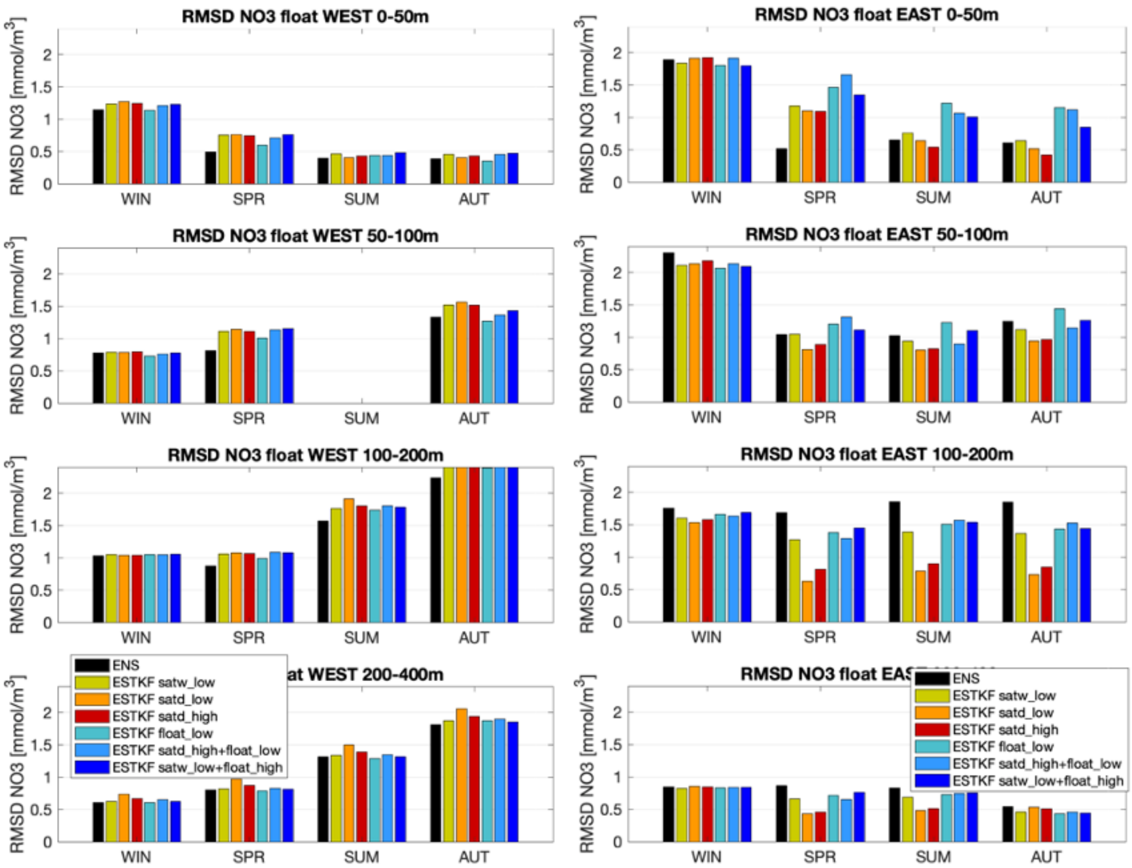

Figure 4.1.4: Nitrate RMSD with respect to BGC-Argo float data for selected vertical layers (0-50m: first row; 50-100m: second row; 100-150m third row; 200-400m fourth column) for the WEST (left column) and EAST (right column) Mediterranean location runs.

Diagnostics on observed and non-observed variables in the 3D Med MFC domain

In the 3D Mediterranean MFC simulations, the SEIK assimilation reduces the ensemble standard deviation at each assimilation step. The ratio between posterior and prior standard deviation calculated for chlorophyll (Fig. 4.1.5) provides an estimation of the uncertainty reduction of the SEIK OC Argo simulation. Satellite observations promote wide areas of corrections (e.g., wide patterns in Fig. 4.1.5), while more local variations on the standard deviation are observed at float profile locations (e.g., round shape patterns around black points in Fig. 4.1.5). Interestingly, the standard deviation reduction is differently affected by the observations depending on specific phytoplankton functional type and season. For instance, the standard deviation of the large phytoplankton group is more affected by the assimilation in winter than in summer, while the picophytoplankton standard deviation is more affected by satellite observations in summer than in winter.

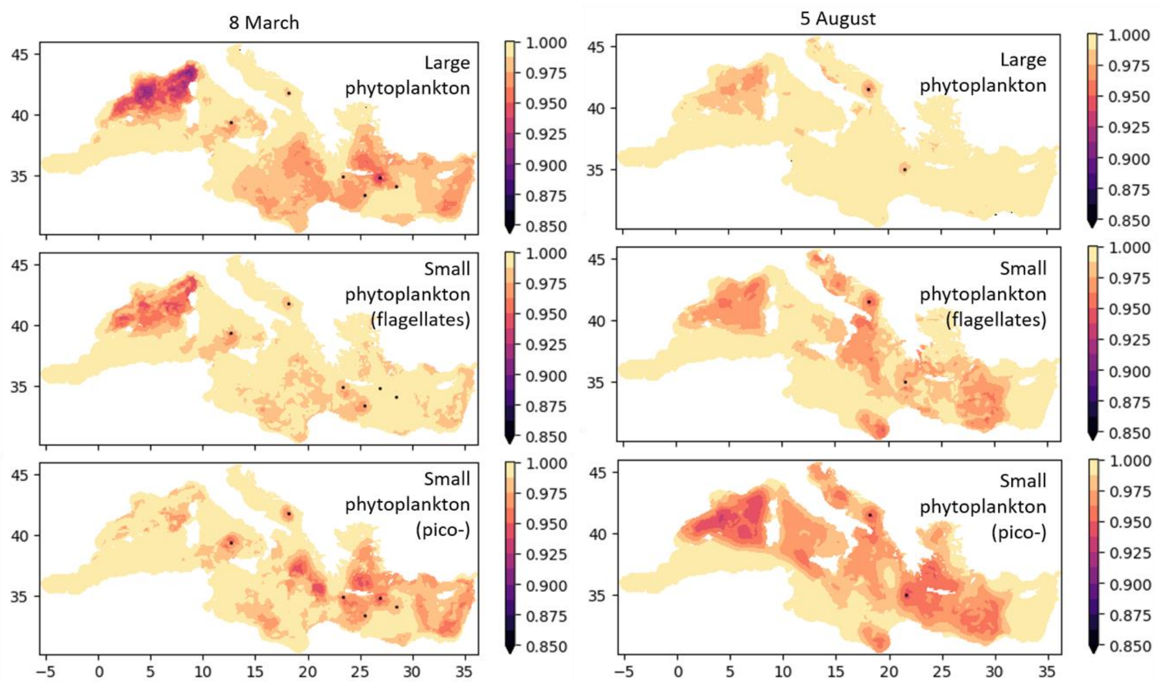

Figure 4.1.5: Ratio between posterior and prior standard deviation of surface chlorophyll in the large (top) and small (middle and bottom) BFM phytoplankton functional types on 8 March (left column) and 5 August (right column).

The assessment of the winter (Feb-Mar 2019) and summer (Jul-Aug 2019) runs of the 3D Mediterranean assimilation is shown in Figures 4.1.6-7 for the observed variable (i.e., chlorophyll) and in Figure 4.8-11 for unobserved variables (i.e., phytoplankton biomass, nitrate, oxygen and POC from BGC-Argo). Additionally, maps of Figure 4.1.12 show the spatial impact of the assimilation of the different types of observations.

The assimilation of surface chlorophyll (SEIK OC) improves significantly the RMSD metrics with respect to OC data in all sub-basins and seasons (Fig. 4.1.6). In particular, RMSD decreases by 40-60% in winter run (Fig. 4.1.6 upper panel), and by 10-40% in summer (Fig. 4.1.6 lower panel). The RMSD decrease in summer is smaller than in winter because of the summer RMSD values are already small and close to the assumed additive-multiplicative error of the observation. The addition of the assimilation of BGC-Argo chlorophyll (i.e., SEIK OC ARGO) does not change substantially the metrics computed on OC data in both winter and summer runs. The RMSDs of the SEIK OC ARGO run are either slightly lower or higher than those of the SEIK OC run.

The assimilation of surface chlorophyll produces a contrasting behaviour on the performance metrics computed on BGC-Argo chlorophyll (Fig. 4.1.7). In fact, chlorophyll RMSD values of SEIK OC improve in the eastern basins while worsen in the western one in the winter run (Fig. 4.1.7 upper panel). Changes are small in the summer run (Fig. 4.1.7 lower panel). The addition of the assimilation of BGC-Argo profiles (SEIK OC ARGO, blue lines) has a positive effect decreasing the RMSD values in all aggregated basins and layers with respect to the SEIK OC run. Improvements are larger in winter than in summer.

As already observed for chlorophyll from BGC-Argo, the assimilation of OC has not a clear positive or negative impact on RMSD of phytoplankton biomass computed on BGC-Argo data (Fig. 4.1.8). However, when the chlorophyll profiles assimilation is added (SEIK OC ARGO), the RMSD generally decreases in all subbasins at surface in both winter and summer runs and decreases in the sub-surface layers of 3 (2) out of 6 (3) subbasins in the winter (summer) run (Fig. 4.1.8). It is worth noting that the impact of profile assimilation is possibly hidden by the daily OC assimilation. Additional tuning would be needed to optimize the impact of the different data-streams.

The impact of chlorophyll assimilation is very small on the skill performance of oxygen computed using BGC-Argo data (Fig. 4.1.9). The addition of profile assimilation does not degrade oxygen. The assimilation of surface chlorophyll does not degrade nitrate dynamics (Fig. 4.1.10, SEIK OC) and the impact of the joint OC and BGC-Argo assimilation (SEIK OC ARGO) on the unobserved variable (Fig. 4.1.10) is satisfactory, provided that RMSD remains substantially unchanged in all subbasins and layers. Using data of bbp700 from BGC-Argo floats, it is possible to assess also the quality of POC in the simulations. Assimilation of surface chlorophyll (SEIK OC) has either positive (e.g., 2 subbasins in winter), negative (e.g., 3 subbasins in winter and 1 in summer) or neutral effects on the quality of POC. The addition of chlorophyll profiles assimilation (SEIK OC ARGO) has a small but always positive impact on the quality of POC metrics (Fig. 4.1.11).

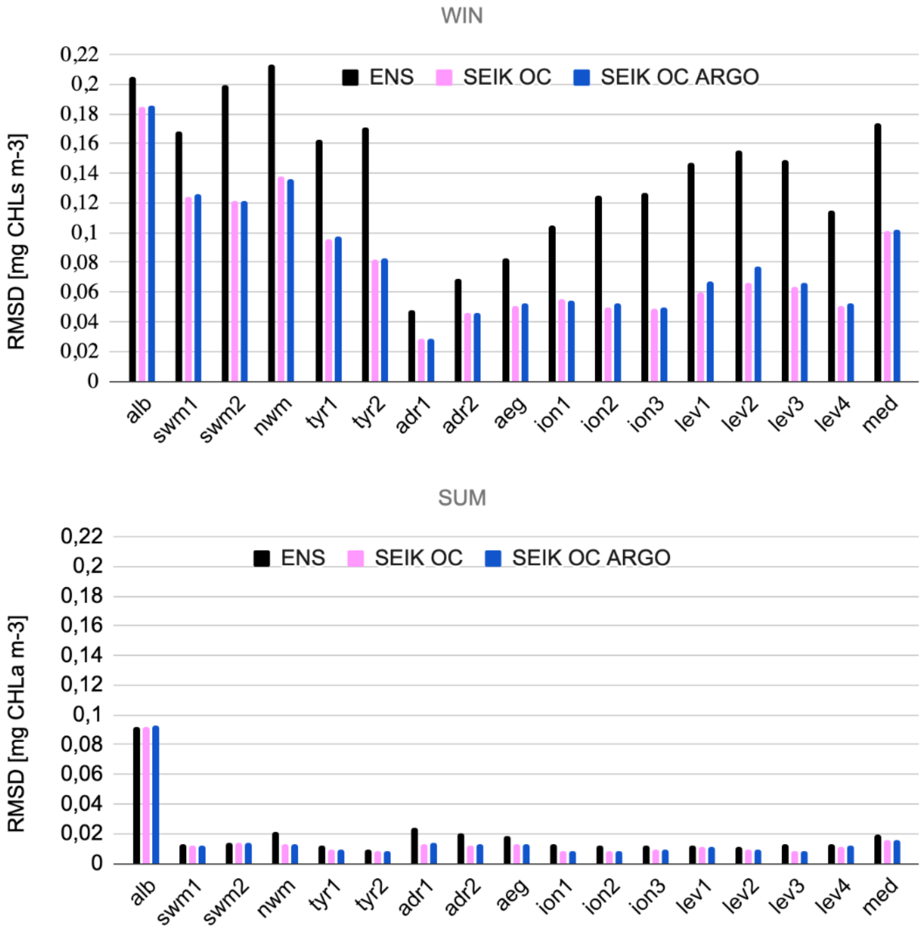

Figure 4.1.6: chlorophyll RMSD with respect to OC data in the 16 sub-basins (see Fig. 4.1.1 for sub-basin definition) for the ensemble free run (ENS, black), SEIK assimilating satellite data (SEIK OC, violet) and the SEIK assimilating satellite and BGC-Argo data (SEIK OC ARGO, blue). Winter simulation (WIN, upper panel) and summer simulation (SUM, lower panel).

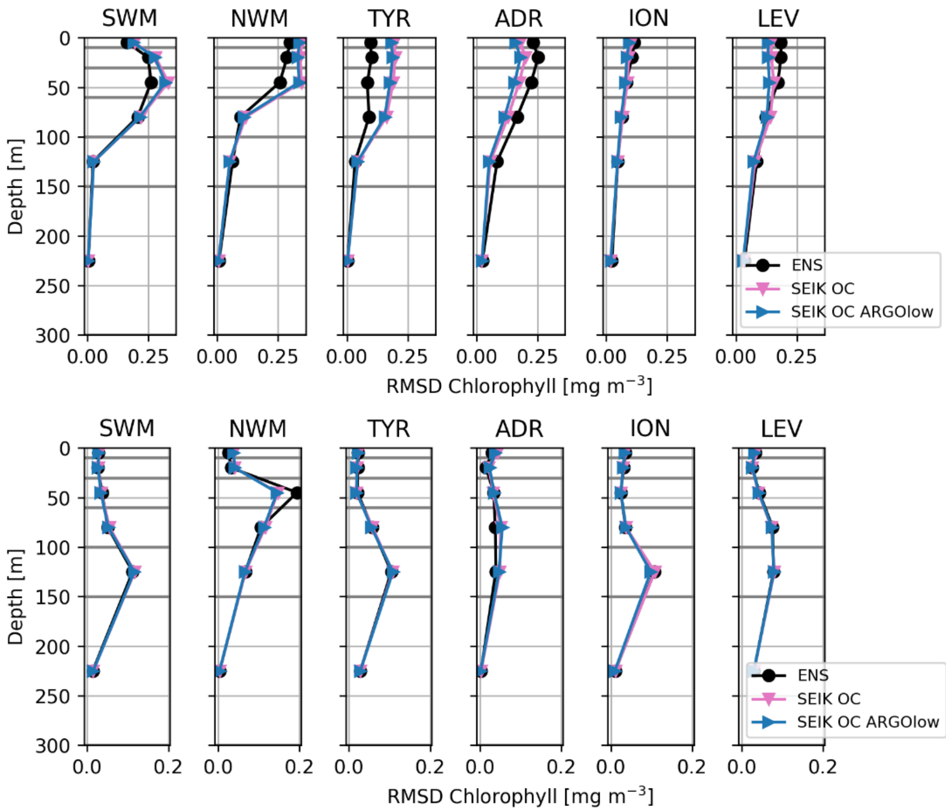

Figure 4.1.7: chlorophyll RMSD with respect to BGC-Argo data in 6 aggregated basins (swm=swm1+swm2; nwm, tyr=tyr1+tyr2; adr=adr1+adr2; ion=ion1+ion2+ion3; lev=lev1+lev2+lev3+lev4) for the ensemble free run (ENS, black), SEIK assimilating satellite data (SEIK OC, violet) and the SEIK assimilating satellite and BGC-Argo data (SEIK OC ARGO, blue) for winter (WIN, upper panel) and summer (SUM, lower panel).

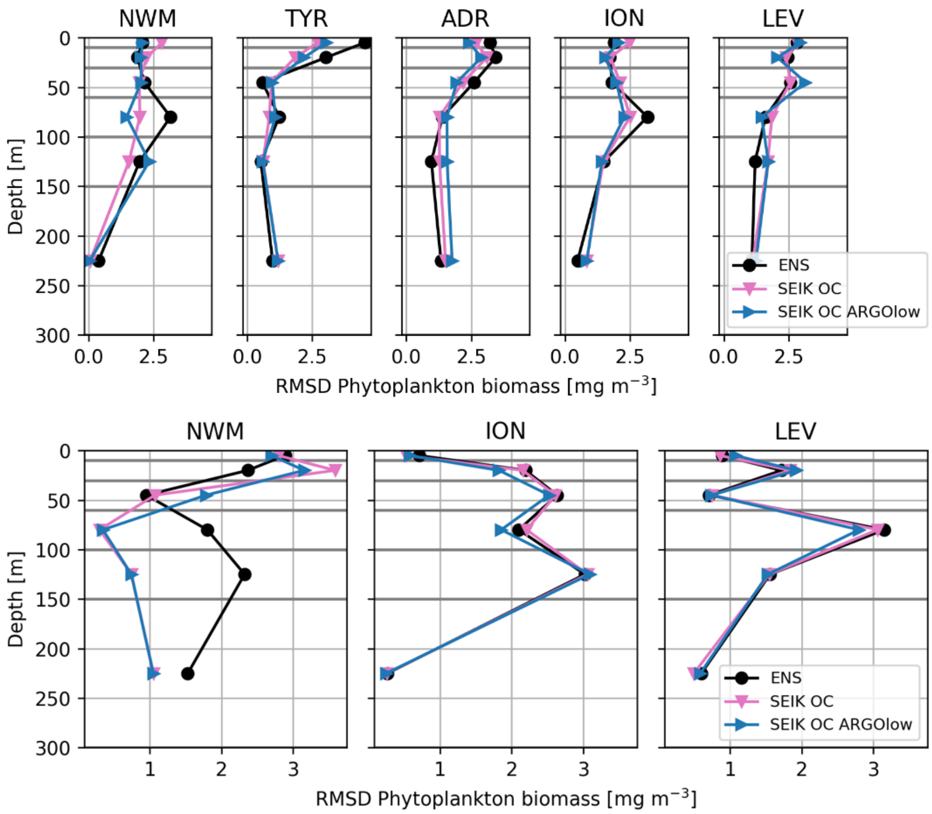

Figure 4.1.8: as Fig. 4.1.6 but for biomass of phytoplankton [mg m-3]. Winter (WIN, upper panel) and summer (SUM, lower panel) experiments.

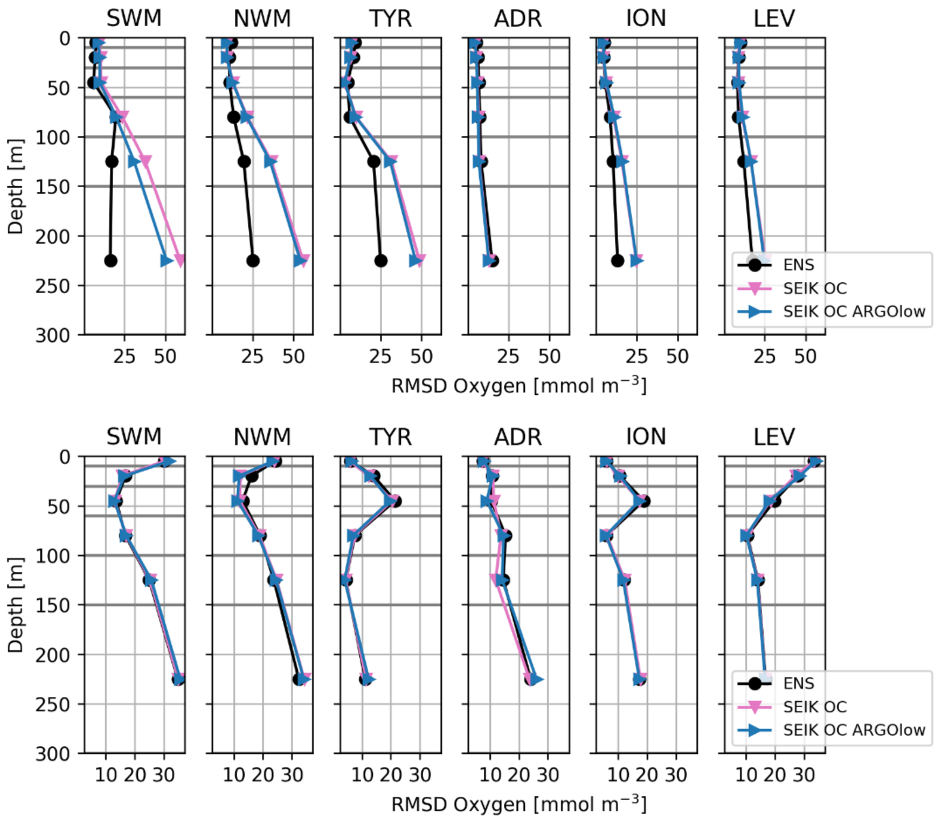

Figure 4.1.9: as Fig. 4.1.6 but for oxygen [mmol m-3]. Winter (WIN, upper panel) and summer (SUM, lower panel) experiments.

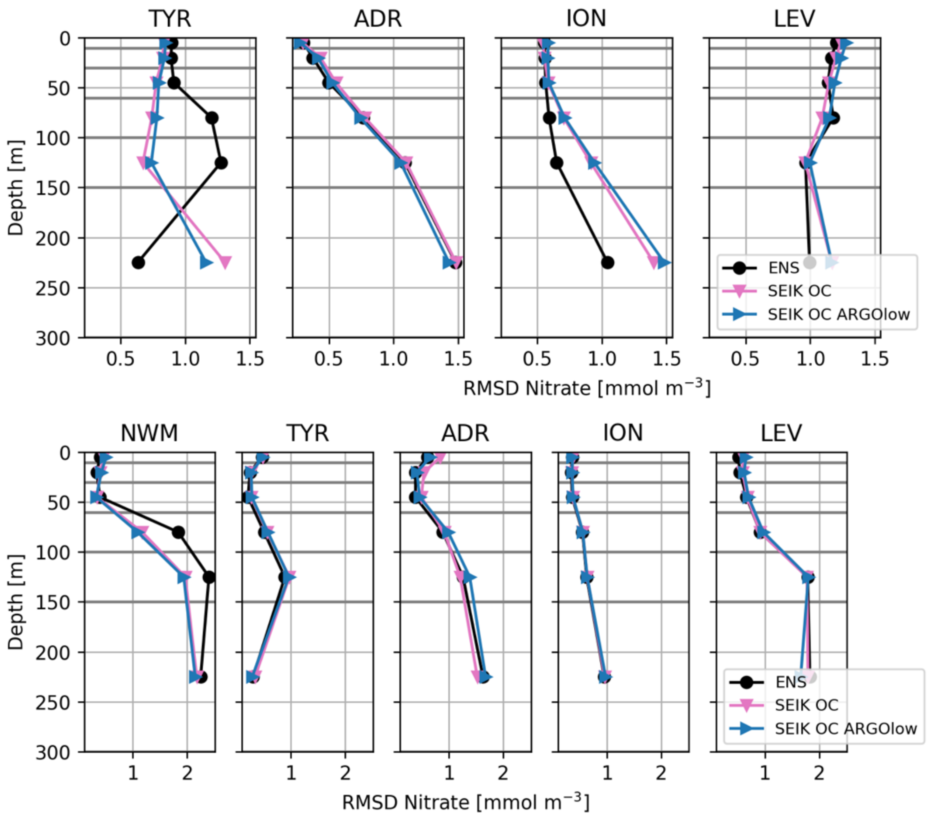

Figure 4.1.10: as Fig. 4.1.6 but for nitrate [mmol m-3]. Winter (WIN, upper panel) and summer (SUM, lower panel) experiments.

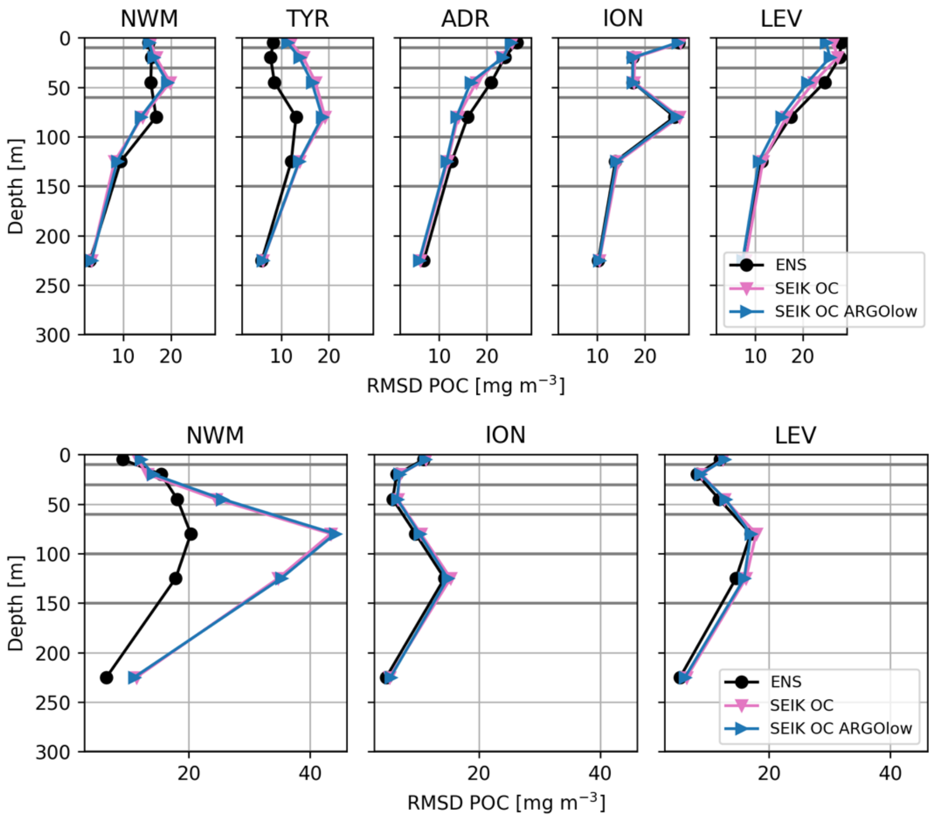

Figure 4.1.11: as Fig. 4.1.6 but for POC [mg m-3]. Winter (WIN, upper panel) and summer (SUM, lower panel) experiments.

Figure 4.1.12 shows the spatial impact of the chlorophyll assimilation for the two different data-streams. During the winter period (when phytoplankton dynamics are mainly confined in the surface mixed layer; left column in Fig. 4.1.12), the impact of BGC-Argo assimilation appears small and hidden by the assimilation of the OC data. In fact, the map of Figure 4.1.12 shows that the largest difference between assimilative runs and the reference is due to the OC assimilation and that the changes due to BGC-Argo (third row in Fig. 4.1.12) are small and close to the float trajectories. During summer period corrections due to satellite and BGC-Argo profiles assimilation can be quite similar in the areas close to the float trajectory at the DCM layer (right column in Fig. 4.1.12) while satellite corrections prevail at the surface layer (not shown). As a result of the temporally evolving spatial covariances and model dynamics, the spatial impact of BGC-Argo profiles assimilation has generally irregular patterns, and it can extend quite far from the float trajectories and are larger in winter than in summer.

It is interesting to note that the effects of ARGO assimilation can be of opposite sign with respect to the ones of OC assimilation (e.g., some of the patches of the third row have opposite sign with respect to the second row - Fig. 4.1.12 -). This indicates that the assimilation scheme can successfully handle possible inconsistencies between the two observation types without destructive effects.

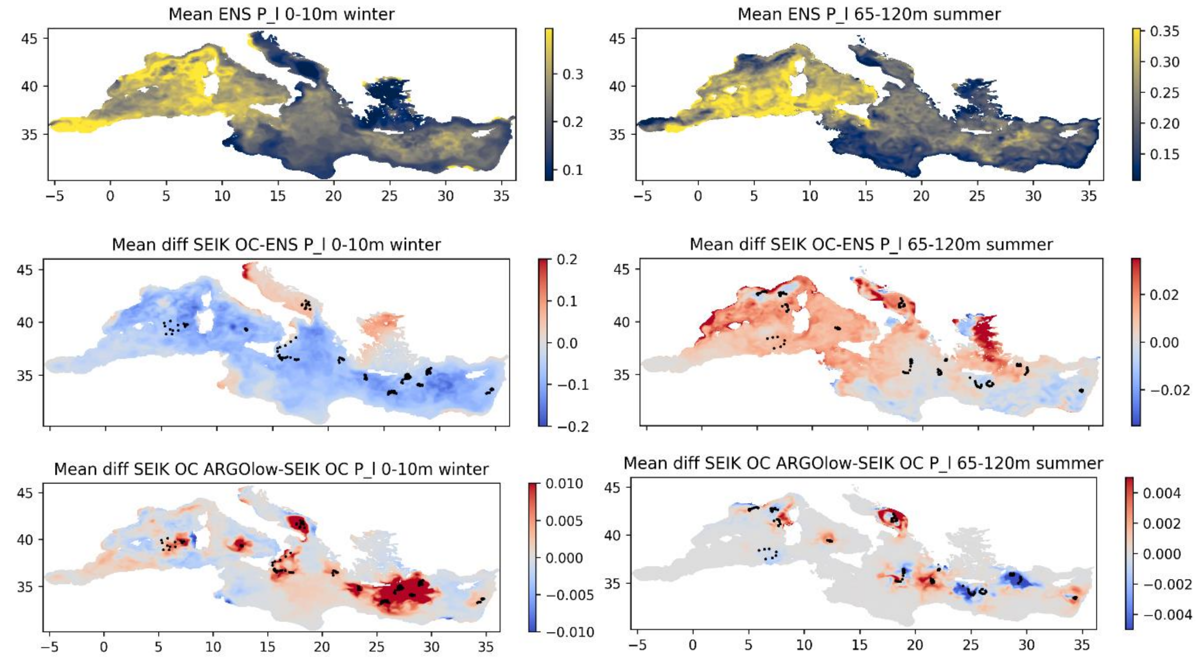

Figure 4.1.12: Maps of mean chlorophyll ([mgCHL m-3] first row), map of mean difference between SEIK OC and ENS run ([mgCHL m-3], second row) and between SEIK OC ARGO and SEIK OC ([mgCHL m-3], third row) for chlorophyll for the surface layer in winter (left column) and the DCM layer in summer (right column). Position of the BGC-Argo floats are reported as black dots. Each map has its own range of colour scale to highlight the patterns.

Diagnostics on the SEAMLESS indicators in the 1D MFC domain

The figures 4.1.13-4.1.16 show the impact of the different assimilation options on the ecosystem indicators. The impact is evaluated in terms of relative variation of the ensemble mean and spread with respect to the ENS runs for the 0-200m layer and for two selected periods. Winter (Jan-Apr) represents the surface bloom period, while summer (Jun-Sep) represents the stratification period when subsurface dynamics are prevailing. The impact is evaluated for the two float locations.

Figures 4.1.13 and 4.1.16 show that indicators that are direct function of the phytoplankton biomass (primary production and PFTs) present a reduction (larger in winter) of the ensemble uncertainty in both locations. On the other hand, indicators that depend on phytoplankton through the model integration (such as flux of POC export from the euphotic zone and trophic efficiency) show either reduction and increase of ensemble uncertainty (Fig. 4.1.15) without a regular pattern.

All assimilation runs reduces the primary production of 10-15% in winter with the largest impact for the satellite-only and low error assimilation (satd_low). In summer, the two locations behave differently, and, interestingly, the multiplatform assimilation (ESTKF satd_high+float_low) reverses the impact with respect to satellite-only assimilation, highlighting the potential importance of chlorophyll profiles to constrain the primary production occurring in the subsurface layer.

Trophic efficiency shows changes in the range of –5 +10% without regular pattern in the different locations and seasons. Export of POC can be greatly impacted by chlorophyll assimilation. Multiplatform assimilation has larger impact than satellite-only in the eastern location while the western location shows no relevant difference among the different types of observation and assimilation options. The PFT indicator appears to benefit from the assimilation of chlorophyll mostly in winter when all assimilation run predict a reduction of the role of large phytoplankton groups. The role of chlorophyll-profile assimilation appears to reduce the correction provided by the satellite-only assimilation. In summer, when the role of large phytoplankton is lower, the assimilation produces lower impact and satellite-only and profiles assimilation can behave in a opposite way (east location in Figure 4.1.16).

It should be noted that these results are only indicative of whether a particular indicator may be affected by assimilation of different data streams, as the specificity of the BGC-Argo sites may prevent generalization of the results.

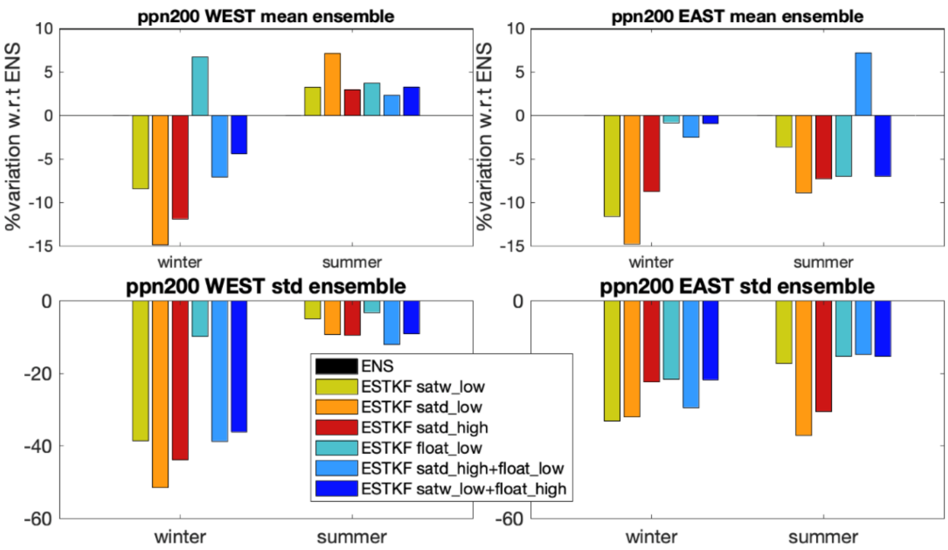

Figure 4.1.13: relative variation of the ensemble mean and spread with respect to the ENS run for 0-200m vertically integrated primary production. The variation is evaluated for two selected period: winter (Jan-Apr) and summer (Jun-Sep).

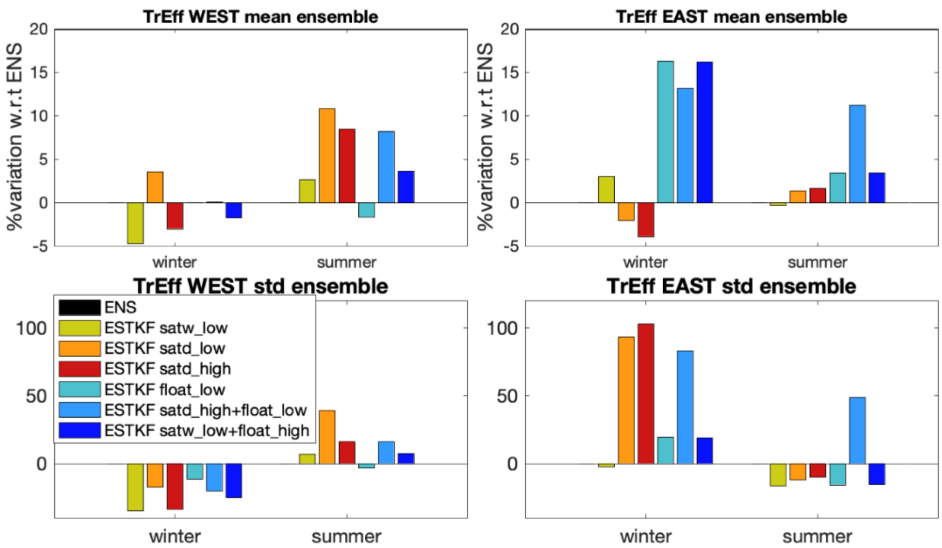

Figure 4.1.14: As in Fig. 4.1.12 but for the trophic efficiency which is measured as ratio between zooplankton and phytoplankton biomasses.

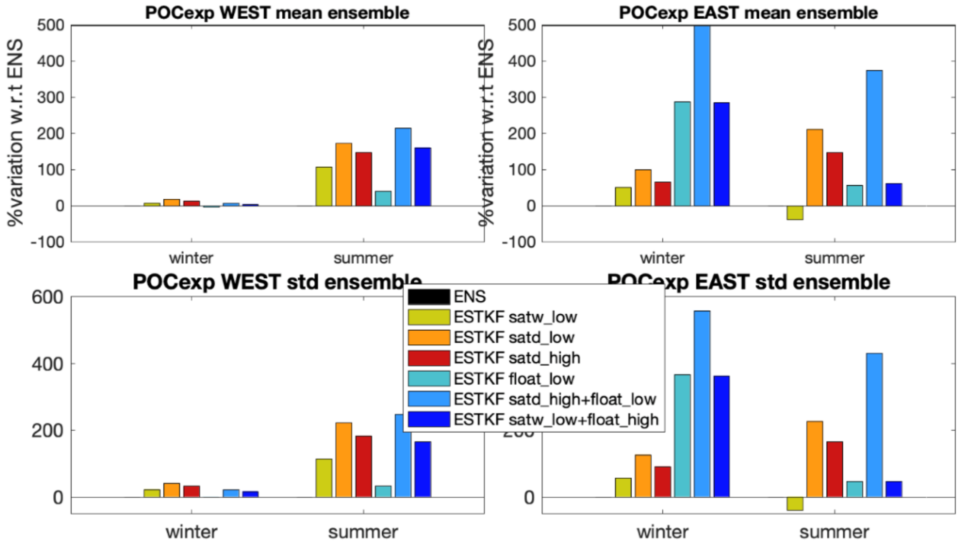

Figure 4.1.15: As in Fig. 4.1.12 but for the export of POC at 500m depth.

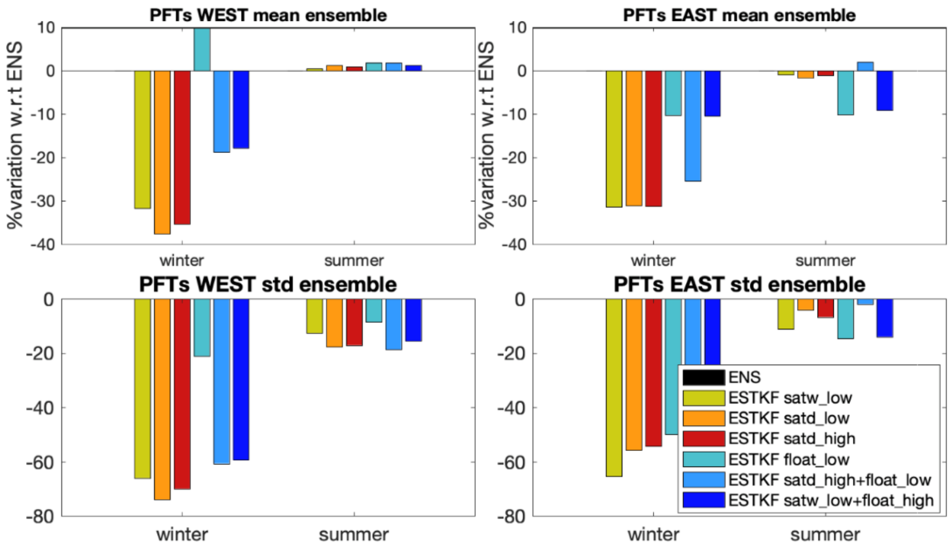

Figure 4.1.16: As in Fig. 4.1.12 but for the phytoplankton functional type, which is computed as the ratio between large phytoplankton and total phytoplankton biomasses.

Diagnostics on the SEAMLESS indicators in the 3D MFC domain

Figures 4.1.17-4.1.20 show the impact of ocean colour (SEIK OC) and joint ocean color and BGC-Argo (SEIK OC ARGO) assimilation on the ecosystem indicators in the Mediterranean domain for the winter and summer runs. The impact is evaluated in terms of relative variation of the ensemble mean with respect to the ENS runs for two selected periods. Winter (Feb-Mar) represents the surface bloom period, while summer (Jul-Aug) represents the stratification period when subsurface dynamics are prevailing.

The OC assimilation produces a general reduction of primary production in winter (first row, right column of Fig. 4.1.17) and varying pattern (positive in western Mediterranean and marginal seas, and negative in Levantine and Ionian seas) in summer (first row, right column of Fig. 4.1.17). The addition of BGC-Argo profiles assimilation has a small absolute impact on primary production (i.e., values of

SEIK OC ARGO and SEIK OC differences are smaller with respect to those of SEIK OC and ENS). However, the differences are often of opposite sign with respect to the OC-only assimilation. The impacts are generally localized close to float trajectories even if signals can be spotted outside float trajectories and with irregular patterns already seen in Figure 4.1.12 for chlorophyll.

In general, the addition of BGC-Argo profiles assimilation produces impacts on the SEAMLESS indicators (Fig. 4.1.15-20) that have spatial patterns similar to those shown for chlorophyll (4.1.11). The impacts of BGC-Argo assimilation are smaller compared with those of SEIK OC in winter. However, they become locally as high as those of SEIK OC in the area close to the float trajectories in the subsurface layer in summer.

Variations produced by BGC-Argo profiles assimilation can have opposite sign with respect to the OC-only assimilation showing that the ensemble scheme and model evolution can handle contrasting information without producing unrealistic solutions.

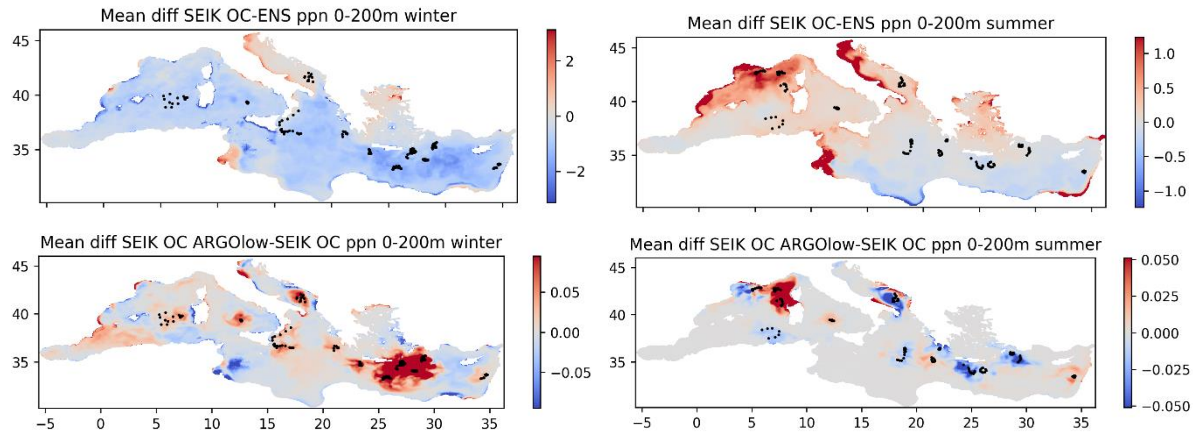

Figure 4.1.17. Differences of the ensemble mean for 0-200m vertically integrated primary production [mg m-3 d-1] between SEIK OC and ENS runs (first row) and between SEIK OC ARGO and SEIK OC runs (second row). The variation is evaluated for two selected period: winter (Feb-Mar, left column) and summer (Aug-Sep, right column). Colour scales of maps are different to spotlight the spatial patterns.

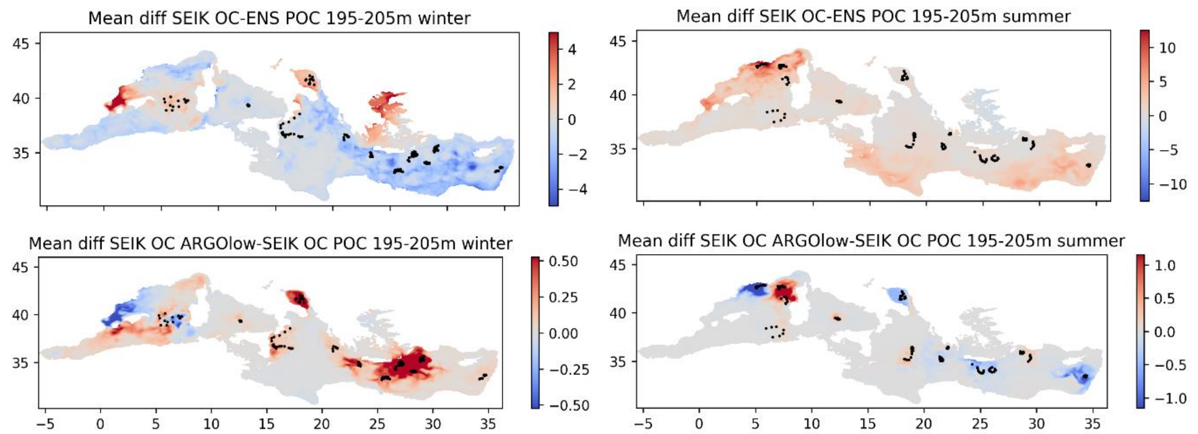

Figure 4.1.18. As in Fig. 4.1.17 but for POC at the depth of 200m [mgC m^{-3}].

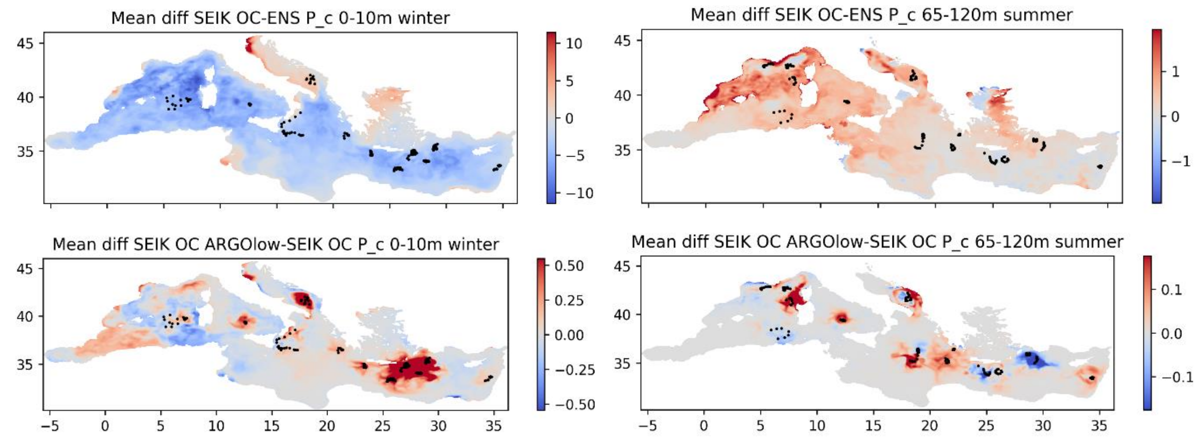

Figure 4.1.19. As in Fig. 4.1.16 but for Phytoplankton biomass [mgC m^{-3}] [mgC m^{-3}].

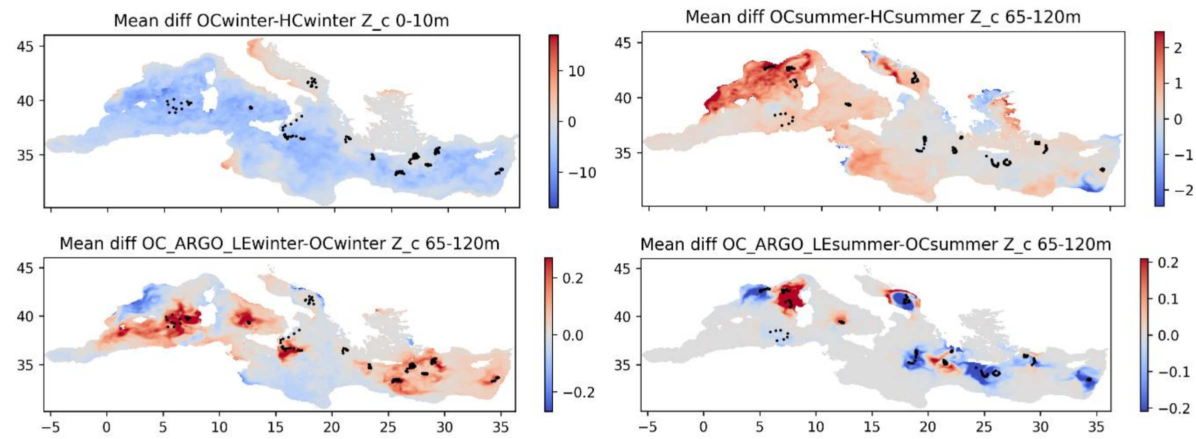

Figure 4.1.20. As in Fig. 4.1.17 but for zooplankton biomass ([mg C m^{-3}] as a proxy for the trophic efficiency.

4.2 Assimilation results in the ARC MFC domain

Results of the ARC system are presented only for the 3D MFC domain since the 1D system didn't provide consistent results to support the development of the 3D MFC domain. Additional work on the 1D system is required to configure the 1D system.

Diagnostics on observed and non-observed variables in the 3D MFC domain

Figure 4.2.1 shows monthly mean surface chlorophyll concentration from April 2019 to July 2019. In general, the current HYCOM-ECOMO coupled model settings for the ARC 3D MFC system produces late and too strong spring bloom in the Norwegian Sea and the North Atlantic subpolar gyre without data assimilation (EX0: FREE RUN). The late onset of the spring bloom is clear from the very weak chlorophyll value in April in EX0. The model bias is corrected after assimilating chlorophyll observation from both in EX1 and EX2. The excessively strong bloom in May and June in EX0 is corrected both in EX1 and EX2. The corrected bloom in May and June is stronger over the majority of the domain in EX2, but the location of the elevated chlorophyll does not necessarily match with the location of the Argo floats (see figure 3.2.2). The impact of assimilating BGC Argo float chlorophyll profiles together with satellite chlorophyll data can be found in Figure 4.2.2. Despite of the float locations being clustered mainly in the eastern Norwegian Sea, the remote effect of assimilating the Argo float data can be clearly seen especially in May and June. Considering that the pattern of the elevated chlorophyll in EX2 is almost identical to the pattern of EX1, it is speculated that this is due to the direct impact of the filter update in the EnKS system rather than a dynamical model adjustment after the filter update. Some elevated surface chlorophyll in EX2, compared to EX1, can be found in July along the East Greenland Sea (EGS) where the free model run tends to produce a too strong bloom. Considering that the pattern and strength of chlorophyll in the EGS is almost identical to EX0, it can be speculated that the impact of assimilating satellite chlorophyll observation is weaker than EX1 after adding Argo float chlorophyll observations, as different types of observations compete with each other. This clear impact of Argo float data in the data assimilation is unexpected considering the paucity of Argo floats (only three to four per assimilation cycle in 2019). Our speculation of the explanation behind this result at this moment is in the settings of observation error for each observation platform set as 30% for satellite observation and 20% for float observation. A clearer understanding, it will require further investigation and experiments.

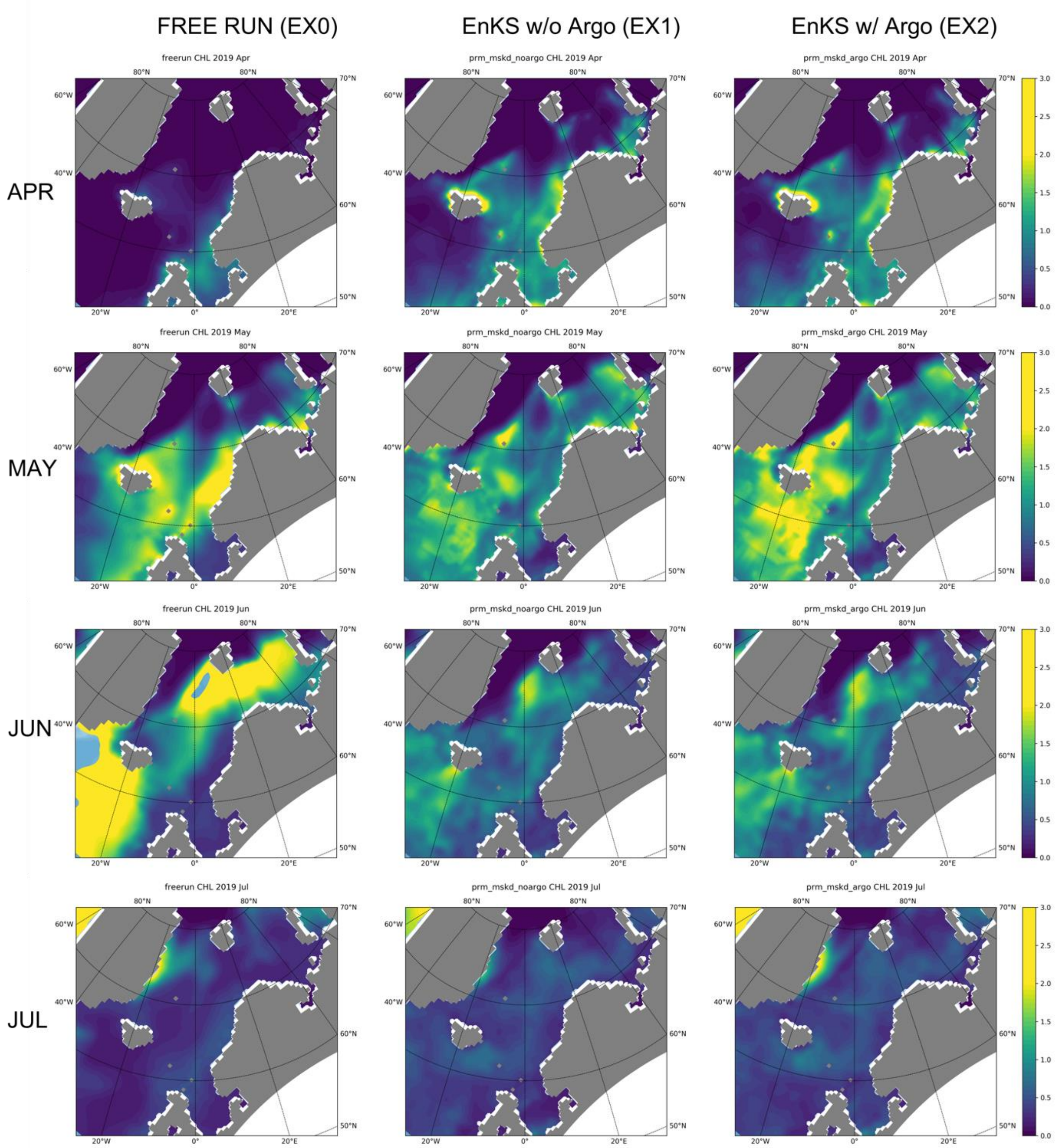

Figure 4.2.1. Monthly mean surface Chl-a concentration [mg Chl/m3] from the three experiments from the ARC 3D MFC system. Left column: model free run, middle column: data assimilation with satellite Chl-a, right column: data assimilation with satellite and BGC Argo float Chl-a. Colorbar range is from 0.0 to 3.0.

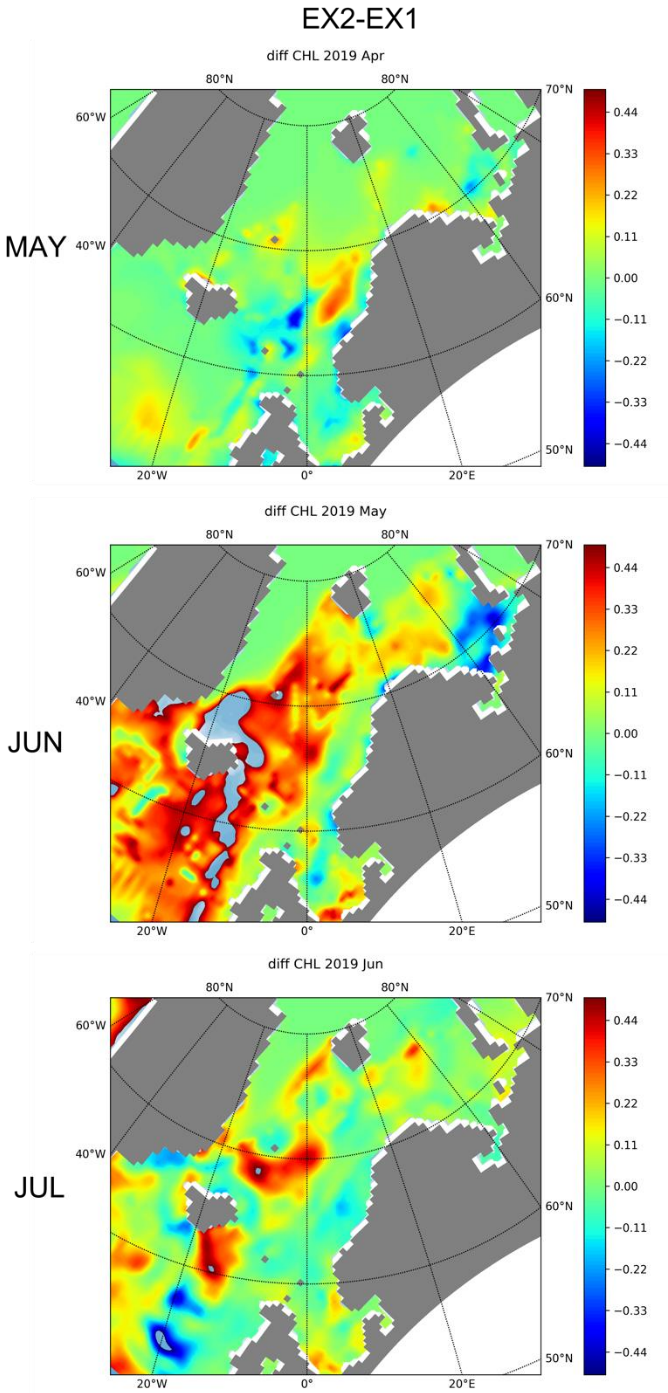

Figure 4.2.2. Difference of monthly mean surface Chl-a concentrations [mg Chl/m3] between two experiments, EX1 (w/o Argo) and EX2 (w/ Argo). Colorbar range is from -0.5 to 0.5.

Diagnostics on the SEAMLESS indicators in the 3D MFC domain

Figure 4.2.3 shows net primary production (NPP) of the surface ocean from the three experiments EX0, EX1 and EX2 with the ARC 3D MFC system. Since NPP is directly associated with the phytoplankton biomass, the impact of Argo float data is similar to what we have observed in the analysis of the surface chlorophyll. The largest impact can be found in the area surrounding Iceland in May when the spring bloom reaches its peak. Figure 4.2.5 shows time series of surface Chl-a averaged over the Norwegian Sea (see Figure 4.2.4) from EX1 and EX2. There is no significant difference in the timing of the onset and length of the spring bloom, but some peaks at cycle 05-17 and 06-18 are larger in EX2 than in EX1. Associated with the peak value change at cycles 05-17 and 06-18, the phytoplankton composition ratio also changes in EX2 at these two peaks. In EX2, the diatom biomass is larger than EX1 (see Figure 4.2.5) which contributes a larger Chl-a in EX2. Thus, the multiplatform DA has impact on phytoplankton functional types (PFTs) in the ARC 3D MFC system. In our 3D system, the surface zooplankton biomass is dominated by meso-zooplankton throughout the experiment. The addition of Argo float Chl-a data has a clear impact on meso-zooplankton biomass and it increases by about 20% through all DA cycles (see Figure 4.2.7). The trophic efficiency (TE) is thus impacted by multiplatform DA in our 3D system.

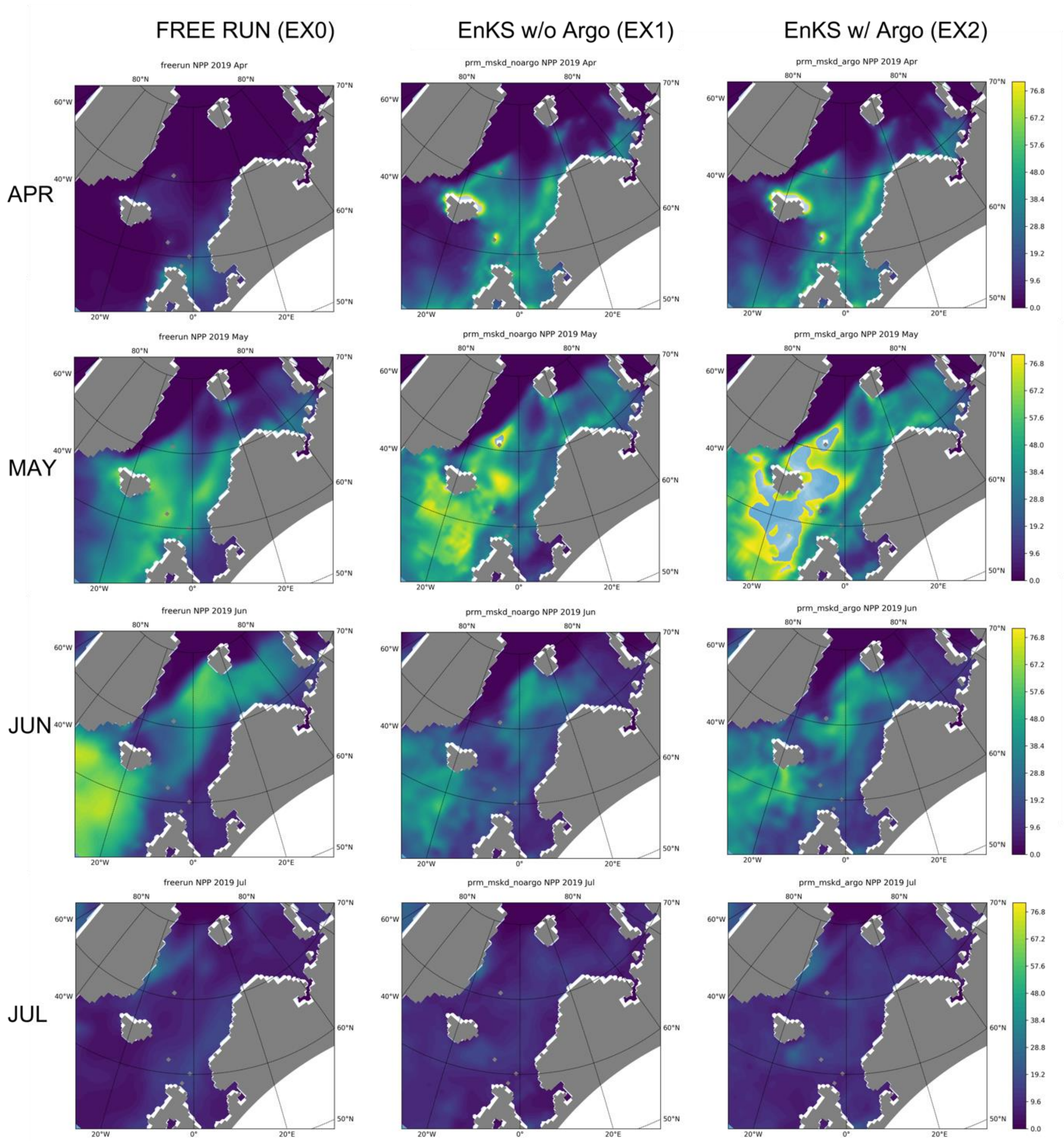

Figure 4.2.3. Monthly mean surface net primary production [mg C/m3/day] from the three experiments from ARC 3D MFC system. Colorbar range is from 0.0 to 80.0.

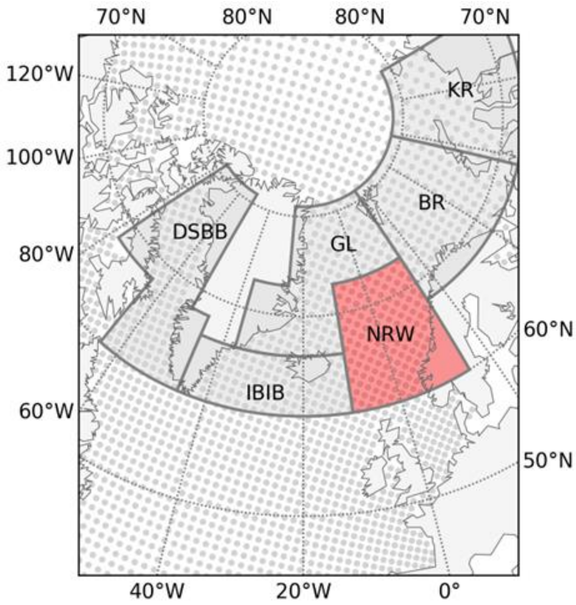

Figure 4.2.4. Norwegian Sea (NRW) validation area in the ARC MFC domain.

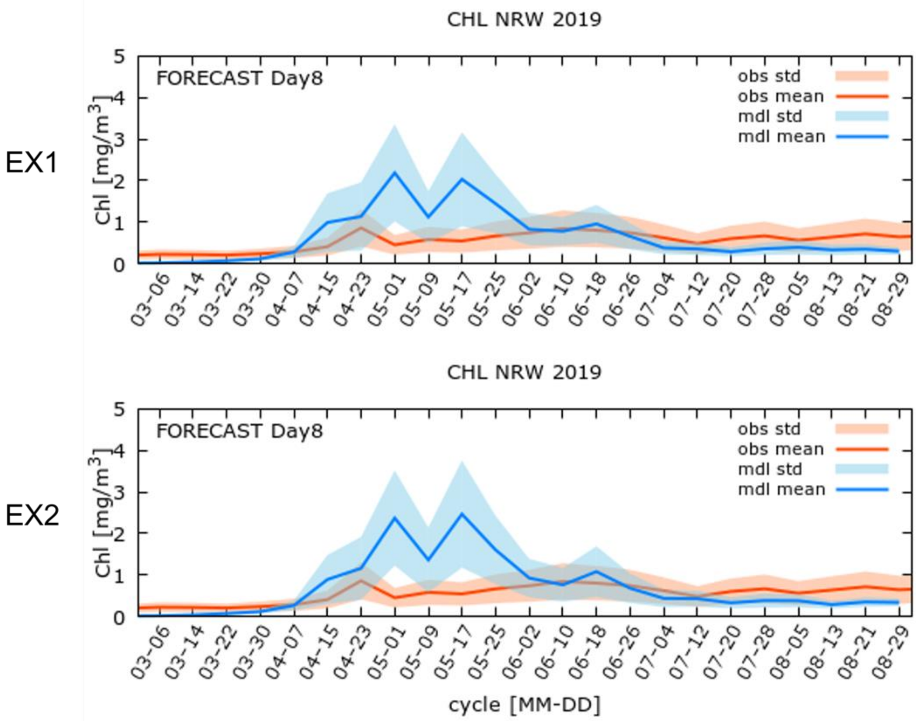

Figure 4.2.5. Ensemble mean (mean) and spread std. (hatch) of surface Chl-a averaged in NRW from EXP1 and EXP2. Blue color is from data assimilation analysis, orange color is from satellite observation.

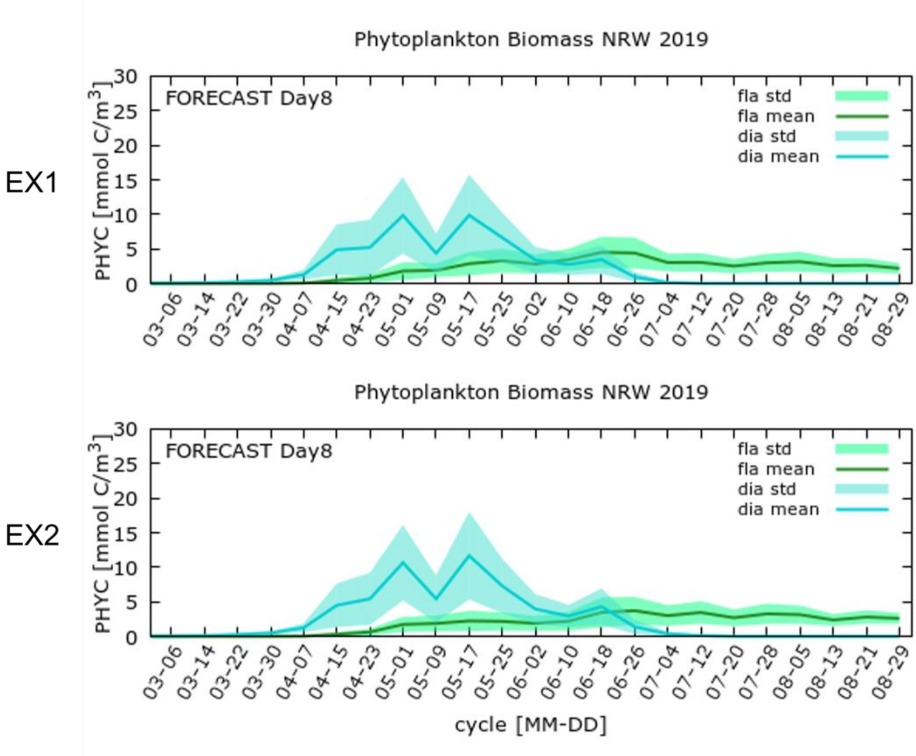

Figure 4.2.6. Ensemble mean (mean) and spread std. (hatch) of surface phytoplankton biomass averaged in NRW from EXP1 and EXP2. Light green is diatom, dark green is flagellate.

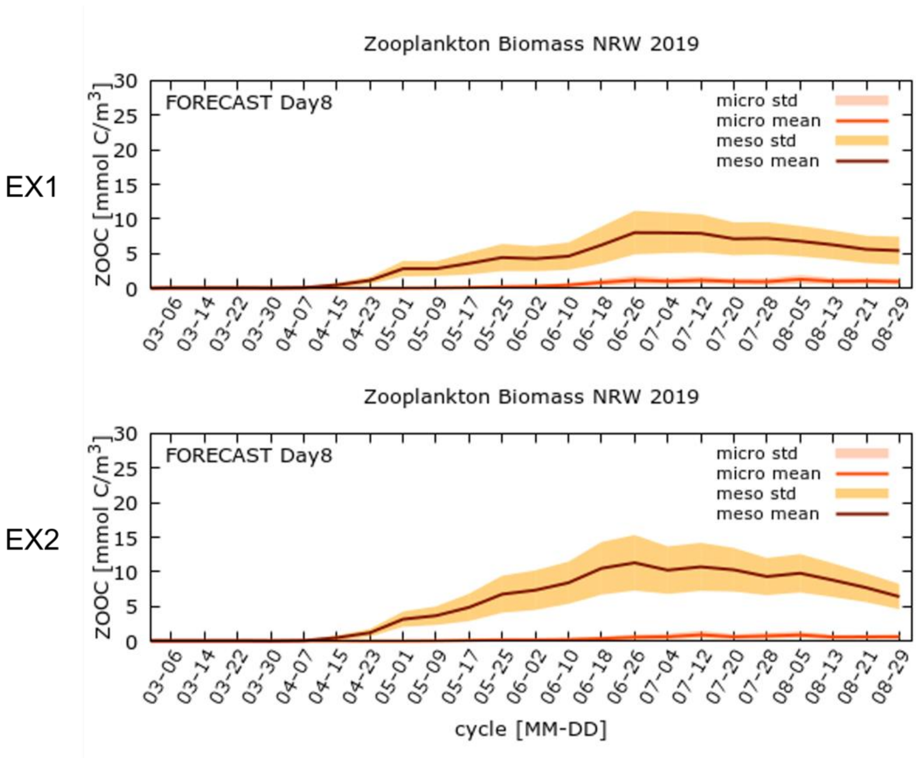

Figure 4.2.7. Ensemble mean (mean) and spread std. (hatch) of surface zooplankton biomass averaged in NRW from EXP1 and EXP2. Dark orange is meso zooplankton, light orange is micro zooplankton.

4.3 Assimilation results in the NWS MFC domain

Diagnostics on observed and non-observed variables in 1D system

The Figures 4.3.1-4.3.3 show that the time frequency of the SST and surface chlorophyll assimilation impacts mostly the ensemble spread representing the uncertainty (Fig.4.3.3), whilst it has much less pronounced impact on the model bias represented by the difference between the ensemble mean and the assimilated reanalysis data (Fig.4.3.2). This is true for both SST and chlorophyll. Since the bias of the model free run is corrected significantly in the November 2014 - March 2015 period (Fig.4.3.1), it seems that the 10-day assimilation frequency is sufficient for improving the model ensemble mean. The uncertainty represented by the ensemble standard deviation is 2-3 times bigger in the run with the 5-day assimilation frequency than in the run assimilating daily time-series, with much lesser difference between the run assimilating data every 10-day and the run assimilating data every 5-th day (Fig.4.3.3). The reduction of ensemble spread during the assimilation step and the growth of ensemble spread between different assimilation steps can be seen in the oscillations within the time-series for the ensemble standard deviation (Fig.4.3.3).

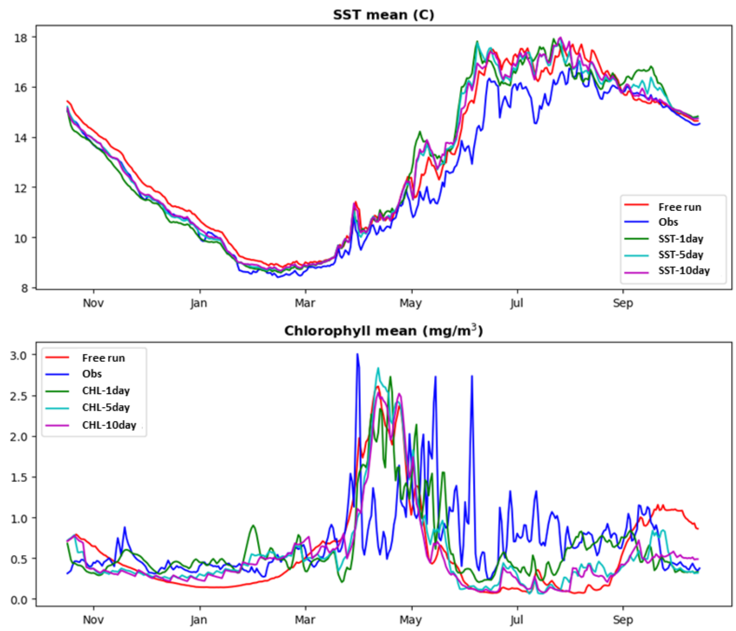

Figure 4.3.1: The experiments comparing the observed variables (SST, chlorophyll) in the assimilation experiments with three different sampling frequencies (1 day, 5 days, 10 days, for the details see Tab.3.3.1), the assimilated data and the free run. The plots of the model runs show the ensemble means.

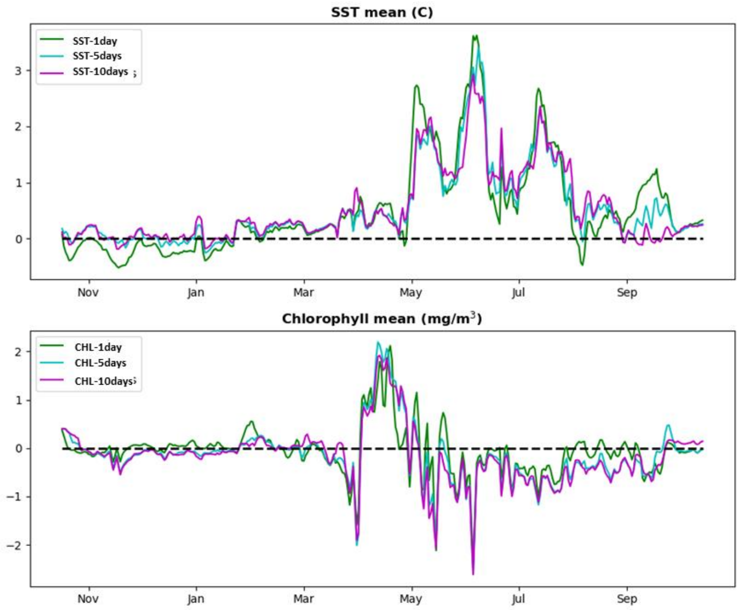

Figure 4.3.2: The same as in Fig.4.3.1 only showing the biases (analysis minus assimilated data) of the three assimilative runs with different sampling/assimilation frequencies.

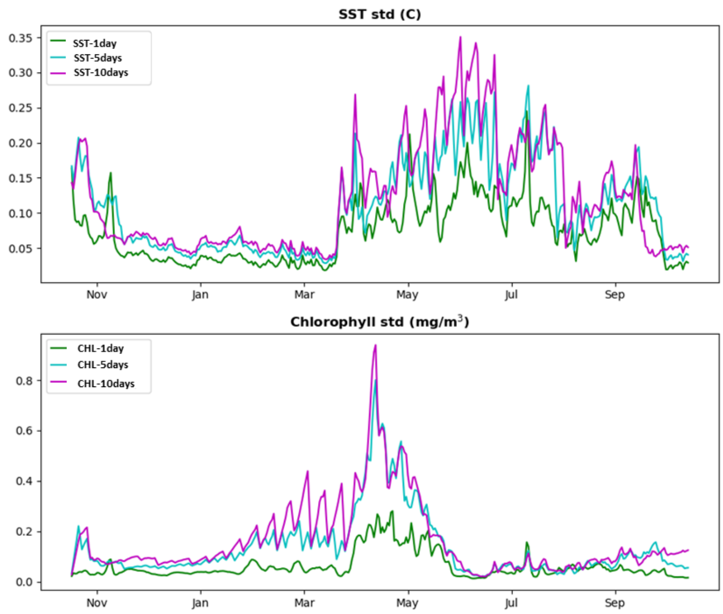

Figure 4.3.3: Comparing the ensemble spread measured by the standard deviation between the three assimilative runs with different sampling frequencies (1 day, 5 day, 10 day) for SST and chlorophyll.

Fig.4.3.4 - Fig.4.3.5 show the experiments assimilating data at different depths. In the mixed period between November 2014 and May 2015, there is no difference between assimilating data at the surface and across the water column. The differences become visible only when the water column becomes stratified during May. In this, from the biogeochemistry point of view, most dynamical period, the surface data assimilation performs relatively poorly (e.g Fig.4.3.1), which is true also about sub-surface data assimilation (Fig.4.3.4-Fig.4.3.5). In general, the greater range of depths at which the

data were assimilated, the better performance of the model, however the overall improvement was in some cases small, whilst significant degradation at specific times and depths could be observed with data assimilation (Fig.4.3.4-Fig.4.3.5). This was true for both temperature and chlorophyll.

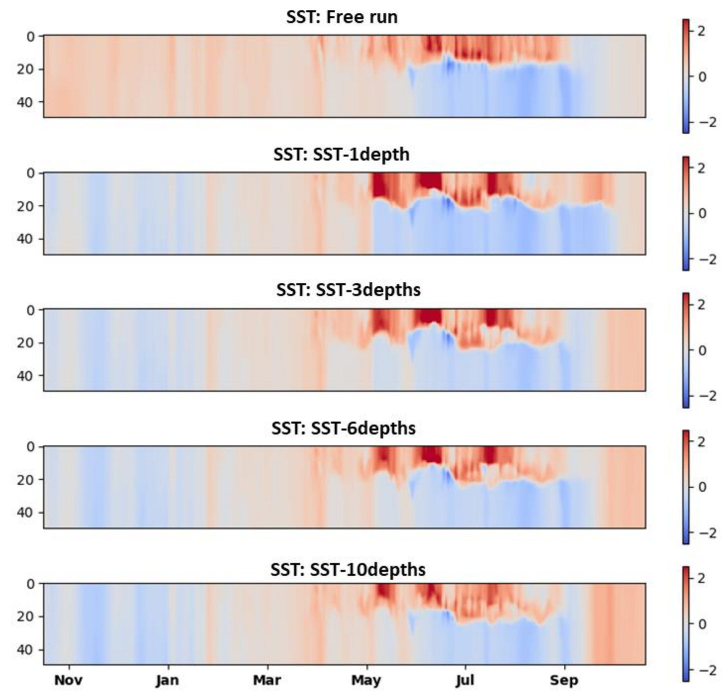

Figure 4.3.4: Hovmoller plots comparing the temperature biases (in C) between the ensemble means of model simulations (free and assimilative runs) and the assimilated Met Office reanalysis data (bias = mean of ensemble minus assimilated data). The different runs are explained in Tab.3.3.1.

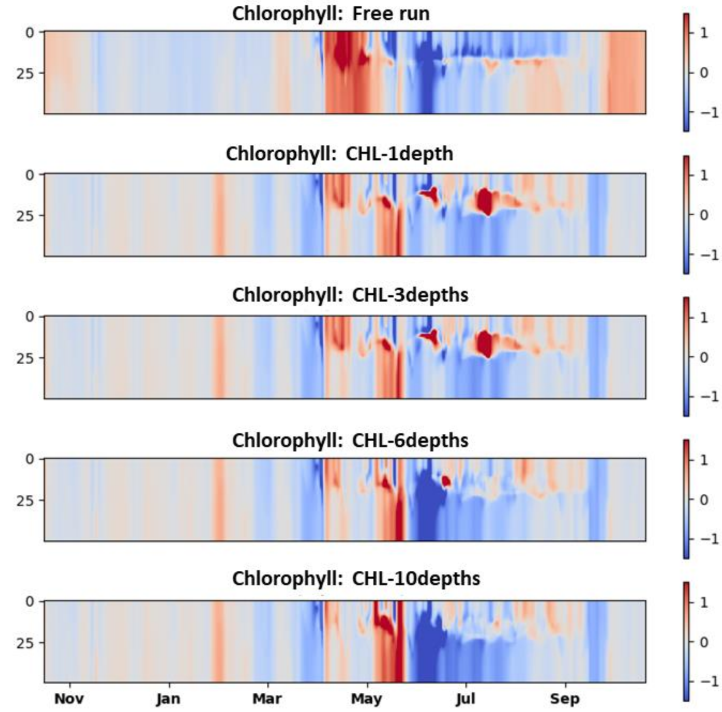

*Figure 4.3.5 The same as in Fig.4.3.4 but for chlorophyll (mg/m**3). The different runs are explained in Tab.3.3.1.*

Finally, Fig. 4.3.6 shows the run assimilating daily reanalysis data for SST and surface chlorophyll, as well as L4 observations for SST, surface chlorophyll and oxygen across the water column. The Figure compares the mean of the model ensemble with the assimilated reanalysis data and the L4 observations. It is clear from Fig.4.3.6 that due to their 5-day frequency the L4 data (as opposed to daily frequency of the reanalysis data), have relatively negligible impact on the assimilation. Although clouds and atmospheric disturbances mean that realistically satellite data will not be available with daily frequency at the same location, in 3D reanalysis there will be typically also satellite data available at neighbouring locations adding to the impact of satellite observations relative to the L4 data. We therefore consider this exercise as reasonable estimate of the impact of the current sampling L4 frequency on the L4 analysis of chlorophyll and temperature.

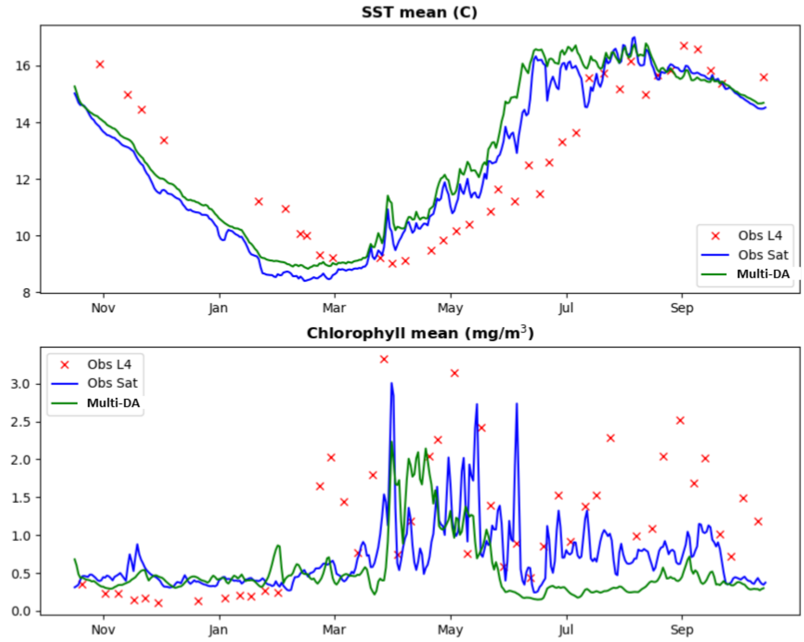

Figure 4.3.6 Comparing the 1D model analysis ensemble mean from the Multi-DA experiment with the assimilated NWES reanalysis data (marked as "Obs sat") and the L4 data.

Diagnostics on observed and non-observed variables in the 3D MFC domain

On the 3D NWS domain the glider chlorophyll assimilation started from February, and Fig. 4.3.7 shows its additional impact, when compared to the reference run, where only satellite data were assimilated. Interestingly, Fig.4.3.7 shows that, far from the area where the glider data were assimilated, there can still be large differences in chlorophyll between the multiplatform DA run and the reference run. It should be emphasized that the horizontal lengthscales in the ensemble-3DVAR system use localization of 4 degrees that prevents creation of spurious long-distance assimilation increments. This, and closer inspection of Fig.4.3.7, indicate that the large differences in chlorophyll across most of the domain in May-June 2018 originate from the propagation of increments from the area of glider observations, and this is despite the fact that the difference between the two runs near the ocean surface gets systematically ``overwritten'' by the satellite data assimilation. This is a very surprising and interesting observation, as it implies (a ``chaos-like'') long term memory in the system, despite the constraints of satellite data assimilation. Understanding better the mechanism behind this phytoplankton memory would be highly desirable. Unlike chlorophyll, oxygen data (Fig.4.3.8) were available already in January and the oxygen-assimilating multi-platform run differs significantly in the glider area throughout the whole January-June 2018 period from the run that assimilated only physics and satellite chlorophyll. Oxygen in ERSEM has only a very weak causal link to other biogeochemical ERSEM variables (Skakala et al 2021), the difference in oxygen between the two runs will not cause differences in other ERSEM state variables. However, both SST and chlorophyll (as proxy of phytoplankton biomass) have very strong causal links to near-surface oxygen and the differences in oxygen throughout the domain in May-June period are most likely caused by the differences in chlorophyll between the two runs.

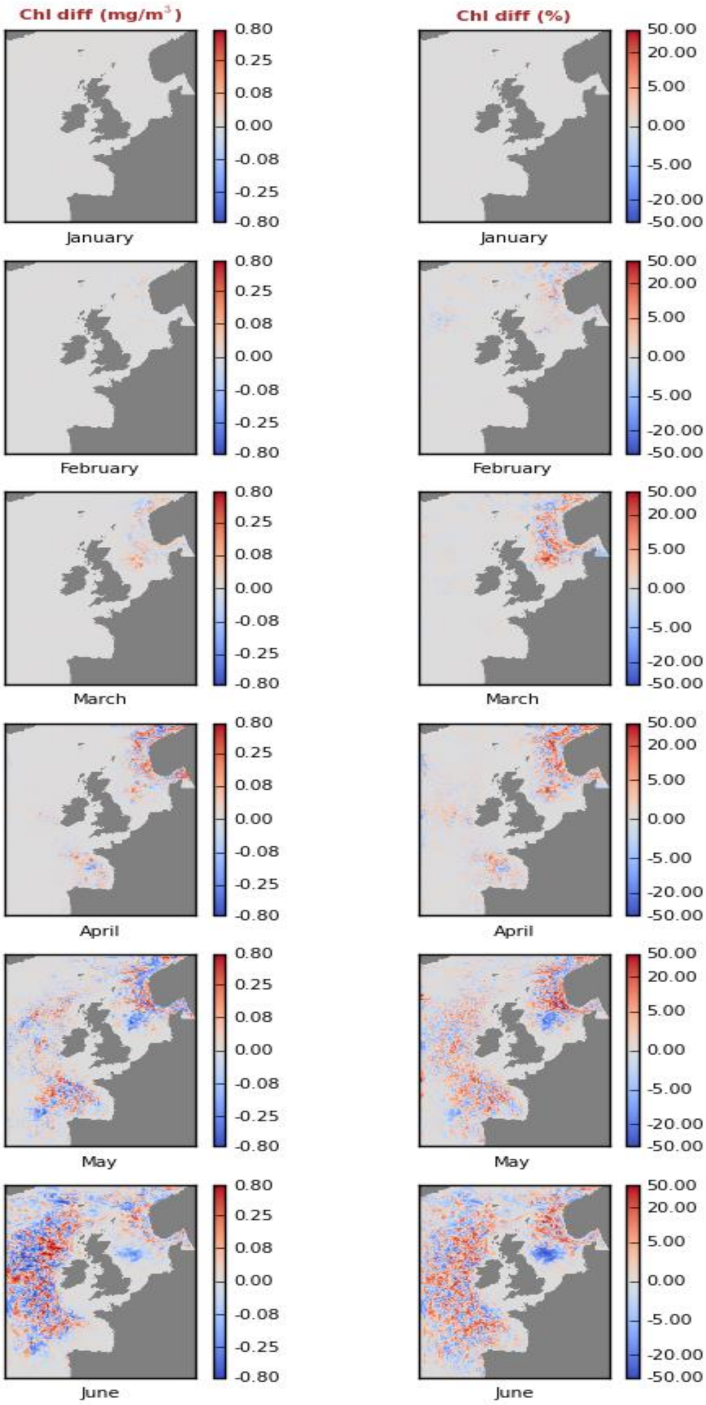

Figure 4.3.7 Impact of the glider chlorophyll assimilation in the multi-platform DA on the NWES during the Jan-June 2018 simulation period. The left-hand panels show the impact in absolute values, defined as an average monthly difference in surface chlorophyll between the multi-platform DA run and the run assimilating only satellite data. The right-hand panels show the same as left hand panels, only relative to the surface chlorophyll value (in %). The different rows show different months.

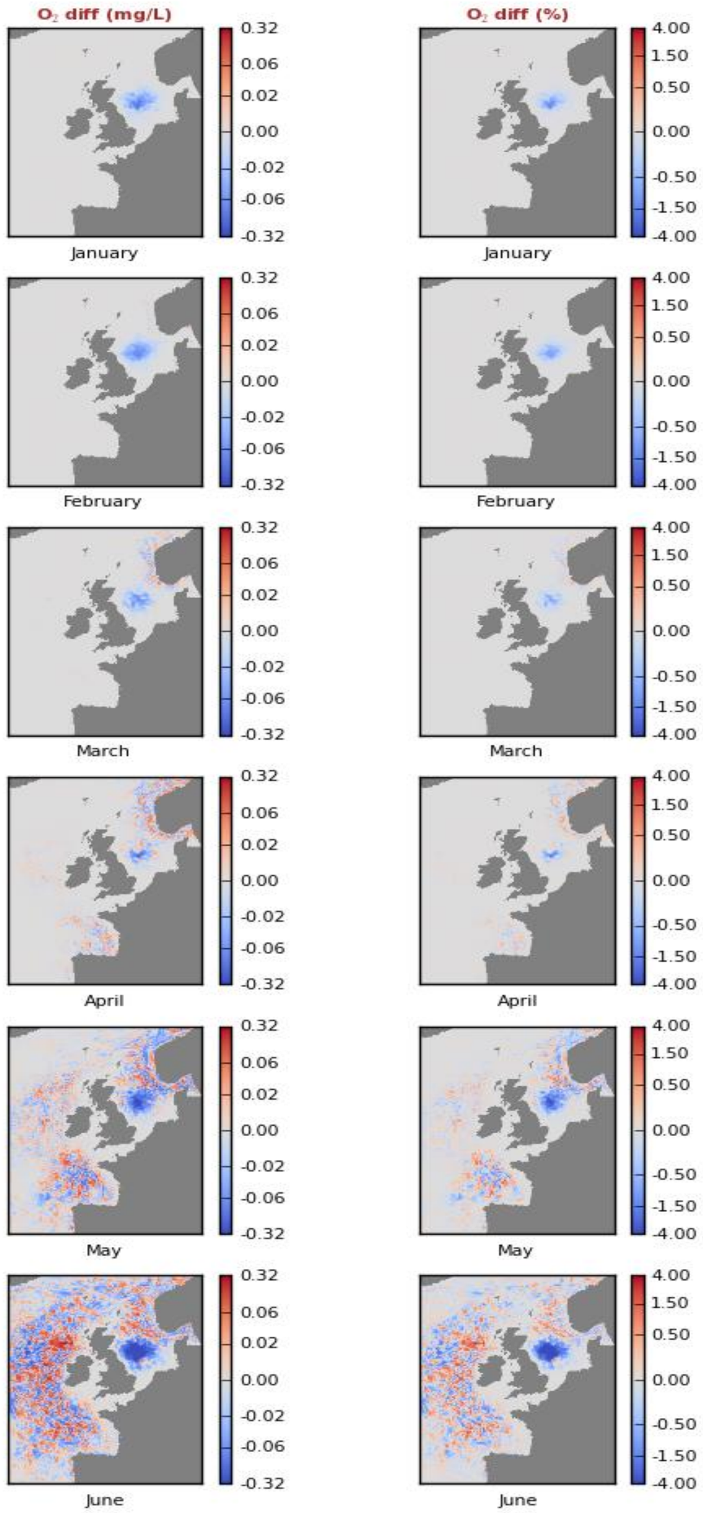

Figure 4.3.8 The same as in Fig.4.3.7, but for oxygen instead of chlorophyll.

Fig.4.3.9 shows the chlorophyll concentrations across the glider trajectory, comparing the glider data with satellite-only assimilation and the multi-platform DA run. It is shown that satellite-only assimilation can produce unrealistic deep chlorophyll maxima (DCMs), which has been already recognized and explained in Skakala et al, 2021. Multi-platform DA largely corrects these maxima and provides a far more realistic chlorophyll concentrations in the deeper part of the water column. The relative improvement by multi-platform DA compared to satellite-only assimilation is shown in Fig.4.3.10, demonstrating that adding glider to the assimilation improves simulated chlorophyll in the vast majority of the water-column (the blue regions in Fig.4.3.10). Similarly, the same is true about oxygen, as shown in Fig.4.3.11.

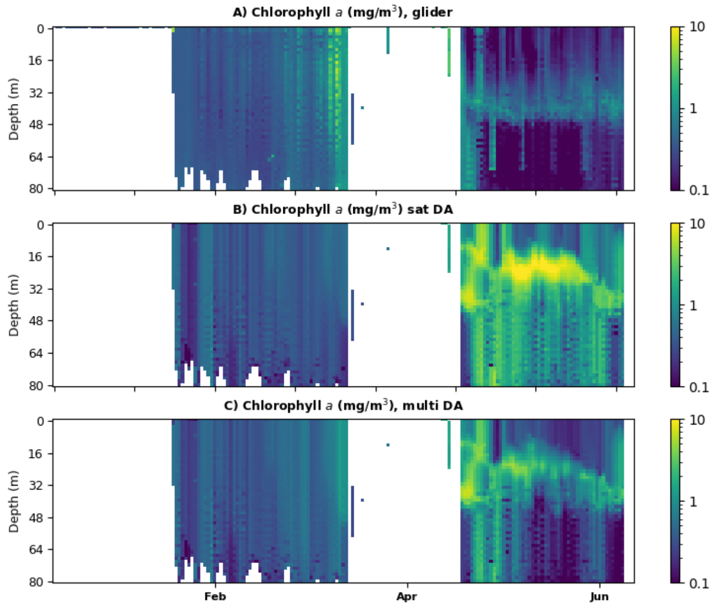

*Figure 4.3.9 Hovmoller plots showing the total chlorophyll concentrations (in mg/m**3) for the glider (upper panel) and the corresponding chlorophyll of the satellite-assimilative run (middle panel), and of the multi-platform DA run (bottom panel).*

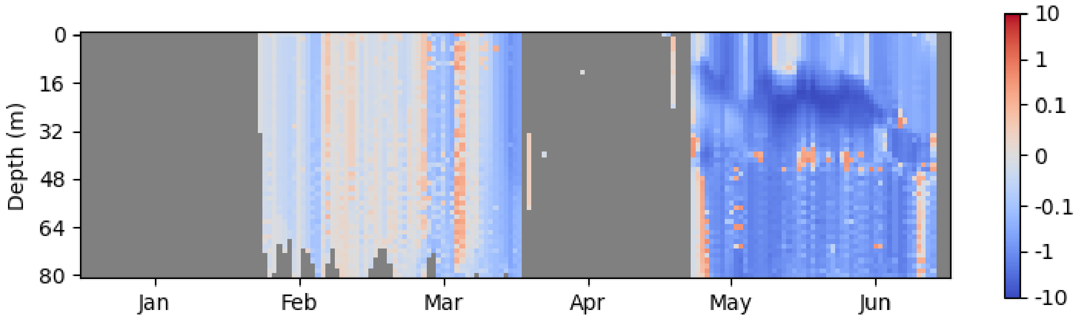

*Figure 4.3.10 Hovmoller plot showing the degree to which glider assimilation reduces model bias with respect to glider data across the glider trajectory. The plot shows the difference in chlorophyll biases (mean of the analysis ensemble minus glider, in mg/m**3) between the multiplatform DA run and the run that assimilated only the satellite data. Wherever the values are negative (blue) the glider assimilation reduced the bias of the analysis, wherever they are positive (red) it increased the bias.*

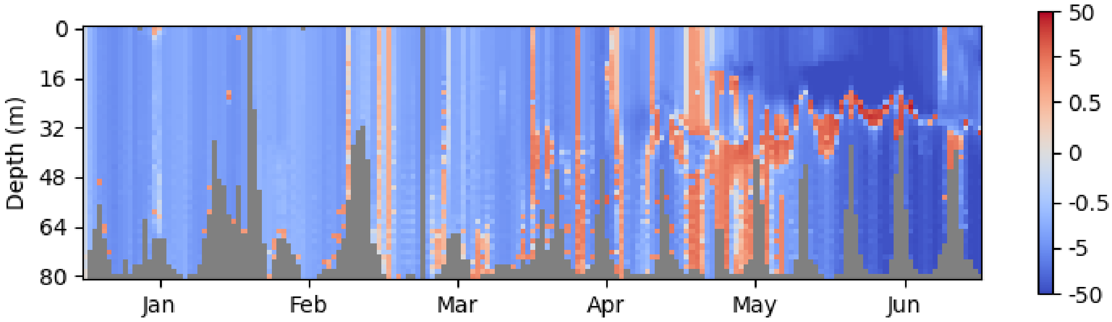

*Figure 4.3.11 The same as in Fig.4.3.10, but for oxygen (mmol/m**3).*

Diagnostics on the SEAMLESS indicators in the 3D MFC domain

Fig.4.3.12 and Fig.4.3.13 show the impact of assimilating glider chlorophyll and oxygen data on the SEAMLESS target indicators: net primary production, bottom oxygen, POC fluxes (Fig.4.3.12) and trophic efficiency, community structure, pH (Fig.4.3.13). The glider chlorophyll assimilation has large impact on net primary production and trophic efficiency, not just in the glider area, but all over the NWES domain (Fig.4.3.12). This is explained by the long memory in the chlorophyll increments propagating through advection of phytoplankton (and most likely a number of additional feedbacks) from the north boundary of the North Sea to the open ocean region in the north-west of the AMM7 domain (Fig.4.3.7). Oxygen assimilation has significant impact on the North Sea bottom oxygen, but this impact is contained to the glider region in the central North Sea (Fig.3.2.2.1). Although the advected phytoplankton impacts oxygen also in the open sea region (see June in Fig.4.3.8), in the deep open ocean this impact stays separated from the sea bottom. Assimilation of chlorophyll from the glider has also a medium impact on the POC fluxes: in the time-constraints of the experiment there is not much change to POC transport in the deep ocean, but there is quite reasonable change within the glider area in the central North Sea, which is 60-100 meter deep. It can be assumed that to see a greater change to POC in the deeper ocean a longer simulation will be needed. Furthermore, glider chlorophyll assimilation has only a weak impact on the phytoplankton community structure. This is presumably the consequence of little PFT community variability within the constrained area of the glider. Finally, the impact of the glider assimilation on pH is very small.

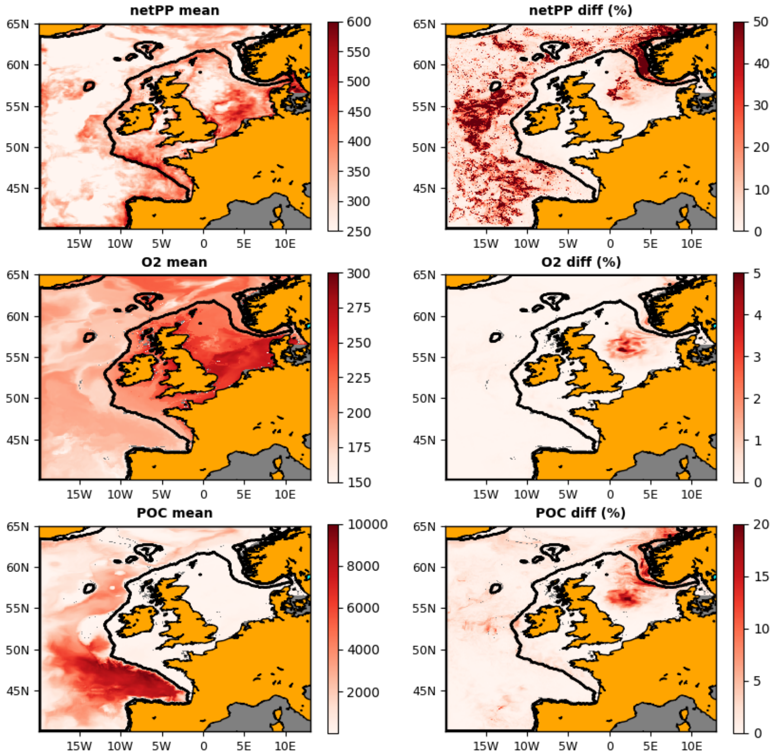

*Figure 4.3.12 Left hand side are the March-June 2018 mean values of SEAMLESS target indicators in the weakly coupled run assimilating physical data and the satellite chlorophyll, whist in the right hand side panels is the March-June 2018 mean relative difference (in %) between the multi-platform run and the weakly coupled run assimilating physical data and the satellite chlorophyll. The indicators are: (i) the depth integrated net primary production (mmol C/(m**2 day)), (ii) near-bottom oxygen (mmol/m**3), (iii) integrated POC (mmol C/m**2) below the 500 m depth, or near the sea bottom, wherever bathymetry < 500m.*

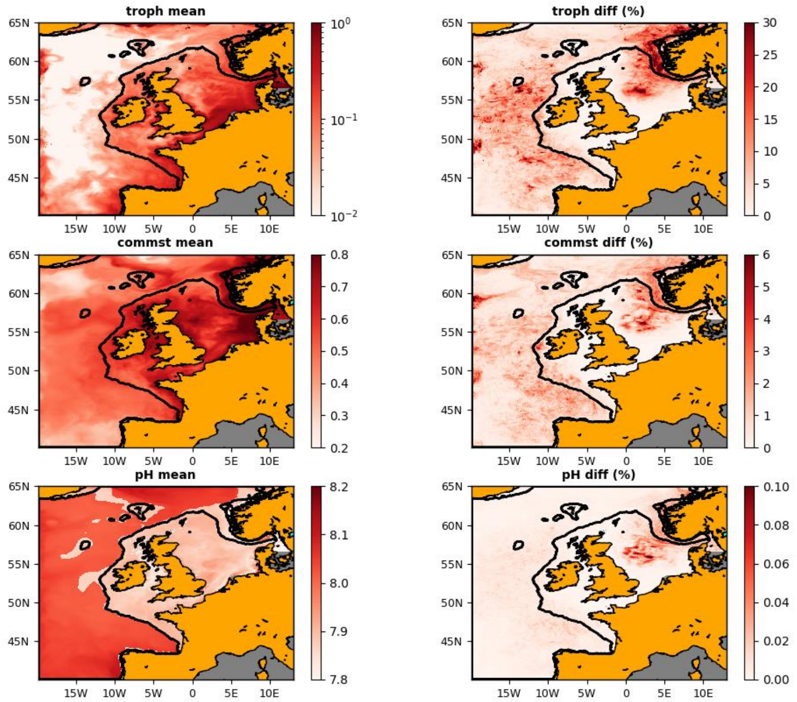

Figure 4.3.13 Similar to Fig.4.3.12, but for the trophic efficiency (depth-integrated total zooplankton carbon / depth-integrated total phytoplankton carbon), the phytoplankton community structure (depth integrated macrophytoplankton carbon / depth –integrated total phytoplankton carbon) and the depth-averaged pH.

Analysis of cost-benefits of multiplatform biogeochemical data assimilation

5.1 Cost-benefits

In this section, firstly we summarize the benefits and computational cost of the multiplatform data assimilation in each MFC investigated. Secondly, we synthetize the results obtained for the SEAMLESS indicators at each MFC emphasize the added values of the joint satellite and profile with respect to satellite-only biogeochemical data assimilation.

5.1.1 MED

Our experiments showed that the joint satellite and in situ data assimilation is feasible in the 3D Mediterranean MFC system even if the impact of SEIK assimilation appears to be generally smaller than that of the 3DVarBio system currently implemented (Teruzzi et al., 2021). Adding profile assimilations to the standard OC assimilation provides improvements on phytoplankton dynamics in sub-surface layers and related ecosystem indicators even when OC assimilation causes degradations. Sensitivity tests performed in the 1D system showed that higher frequency assimilation has larger impacts, and that the profile observations should have lower errors than surface observations to increase the effectiveness of the former data stream. Lessons learnt on 1D setup are not conclusive. Indeed, the transferability of 1D insights to the 3D Mediterranean system is not straightforward given

the importance of the horizontal components of error covariances of model and observations and tuning some specific aspects (e.g., observation errors, forgetting factor) is still required.
The computational cost of the tested 3D ensemble assimilation system is roughly n times (with n equal to the number of the ensemble members) that of the present CMEMS MFC MED-BGC system. Then, in theory, provided that an ensemble system is in place, the assimilation of multiple types of observations should come without additional computational cost above the assimilation of satellite-only data. In practice, given the necessity of the additional tuning, the effectiveness of the multiplatform assimilation can have some limitation. Thus, the actual computation cost of the ensemble OGSTM and the necessity of additional tuning make the ensemble system not ready for its implementation in the operational MED-MFC-BGC system.

5.1.2 ARC

The additional numerical cost of adding BGC Argo float data compared to original ARC 3D MFC settings, in which only satellite chlorophyll data are assimilated, is negligible. This is due to two factors in the current data assimilation settings. The first factor is the paucity of BGC-floats in the ARC MFC domain, 60N and above of the Arctic Ocean and the Nordic Seas. As described in subsection 4.2, the average number of available floats in the domain per one assimilation cycle is 3 to 4 in 2019 and the number was even smaller when the BGC Argo observation program has started in 2011 in the Norwegian Sea. We also do not foresee that the number of BGC Argo floats increase significantly in our analysis domain in near future. The second reason is “superobing” of our data assimilation system in which original data are thinned to match the ocean model grid resolution prior to data assimilation. Due to a relatively coarse model grid setting in the current ARC MFC model, the number of vertical observation levels after superobing is usually less than five per float. This keeps the ratio of effective number of float data against satellite data significantly small and hence reduces the additional numerical cost. In the next version of the ARC MFC system, the vertical resolution becomes double compared the current one. Still, we do not expect a significant increase of the numerical cost in near future from this aspect either. The most noticeable cost of adding float data to the current data assimilation system is the time necessary for tuning data assimilation settings. As is observed in 4.2, assimilating float observation has an excessive impact with regards to the relative coverage of in situ versus satellite observations. This requires a careful tuning of data assimilation parameter settings such as observation error amplitude for each observation platform.

5.1.3 NWS

Adding multi-platform capacity to the ensemble-3DVar set-up whether in 1D, or 3D bears almost no additional computational cost. Adding profiles to assimilation in 3D can have a surprisingly large impact across far larger portion of the NWS domain than the area covered by the glider mission. This could be due to an ocean ``butterfly effect’’ where localized perturbations to the system propagate across domain through both physical advection and coupled physical-biogeochemical nonlinear dynamics. One of the potential routes how this can happen is the two-way coupling between the physical and the biogeochemical model, where the localized perturbations to chlorophyll caused by glider data assimilation can trigger localized perturbations in physics (e.g in water-column stratification), which then spread out along with biogeochemistry across the domain. Various mechanisms behind the temporal and spatial propagation of chlorophyll increments should be better investigated in the future. Furthermore, our 1D results indicate that the high sampling frequency typical for the glider measurements can be perhaps slightly relaxed without much degradation of the analysis skill. The glider assimilation improves the sub-surface chlorophyll and the oxygen in the whole water column, when assessed by comparison with the assimilated glider data. However, the impact of ensemble-3DVar assimilation is generally smaller than of the 3DVar system, shown in Skakala et al, 2021. This is analogous to the results from WP3-WP4, and is expected, as the dynamically modelled background variances by the ensemble are typically smaller than the parametrized (climatological) variances used in the 3DVar system. Which of the two simulations is better, needs to be assessed by longer runs and using large independent observational data sets. So far, our results indicated that the dynamically estimated variances are more realistic, however paradoxically due to their realism they have no longer the capacity to error-compensate some other features of the DA system (e.g detrimental impact of physical DA on chlorophyll). Similarly, we do expect that unlike the 3DVar system (e.g Skakala et al, 2020), the ensemble-3DVar system is far more sensitive to the observational error uncertainties. Thus these (positive) developments (flow-dependent background variances) open the need to address a number of new issues, such as the interplay between physical DA and phytoplankton, or observational data uncertainties, which remained hidden in the 3DVar system. For the moment we recommend using multi-platform DA for reanalyses, however until the ensemble-3DVar system is much better assessed, we would recommend to continue using the current variational system, due to the high cost of ensembles and some of the previously mentioned issues. As for the real-time applications 3DVar multi-platform DA is feasible (e.g Ford et al, 2022), but relies on reasonable data-quality control in real time.

5.2 Surface Chlorophyll, phenology

In SEAMLESS, the **Phytoplankton phenology** consists of three indicators: the value of the maximum of chlorophyll concentration in the layer 0-5m (mgChl m^{-3}), the depth of the maximum of chlorophyll during the summer period (m) and the timing of the bloom, i.e. the time of the year when the two maxima occur (day). (Deliverable D3.2)

5.2.1 MED

Not evaluated because the 3D winter simulation tests were too short.

5.2.2 ARC

From 3D experiments, we observed a medium impact of the multiplatform DA in the surface chlorophyll, phenology. Adding BGC Argo float data does neither change the timing or length of the spring bloom, but its peak value becomes stronger. However, the result indicates that the DA system needs further tuning to make a balance between multiplatform observations.

5.2.3 NWS

Multiplatform DA changes significantly the phenology, also outside of the glider area. The phenology changes can be assessed from the vertical distribution of chlorophyll (Fig.4.3.9) which look much more realistic when glider was assimilated into the model, than when only satellite data were assimilated.

5.3 POC flux

In SEAMLESS, the **Particulate Organic Carbon (POC)** is defined here as the non-living carbon fraction of particulate organic matter, i.e. the detritus, and is computed as the average concentration of the 0- 200m layer from the model output, or 0-bottom in shallower areas. Here we consider the POC flux, i.e. the sinking flux at a depth of 500m (or 200m). (Deliverable D3.2)

5.3.1 MED: Multiplatform assimilation in the 3D domain has a moderate impact on POC fluxes given the effect of profiles assimilation to phytoplankton dynamics in the subsurface layers, particularly during summer. Spatial patterns of changes in the 3D Mediterranean domain reflect those of the chlorophyll changes. Even if POC diagnostics improve, the small number of BGC-Argo floats with bbp700 data prevents a robust generalization of the results.
Additionally, the 1D experiments showed that the uncertainty of the multiplatform DA can increase with respect to both the satellite-only assimilation and the float-only assimilation. It might be possible that the joint assimilation introduces contrasting corrections on phytoplankton dynamics at depth that contribute to increase the variability of POC export.

5.3.1 ARC: Not evaluated

5.3.3 MWS: Multiplatform DA has medium impact on POC fluxes, mostly inside the glider area.

5.4 Primary Production

In SEAMLESS, the **primary production** is the synthesis of organic compounds from dissolved carbon dioxide through photosynthesis as source of energy. Primary production is computed as the vertical integral of the 0-200m layer. The unit is mmolC m^{-2} d^{-1}. (Deliverable D3.2)

5.4.1 MED: Results of multiplatform DA reveal small changes on primary production with respect to the ENS simulation with always a reduction of the spread of the ensemble (e.g., results from the 1D experiments). However, the direction of the change of the multiplatform DA are not always aligned with those of the single observation type assimilation and it might reflect the effect of the inconsistency between OC and surface chlorophyll.

5.4.2 ARC: From 3D experiments, we observed a medium impact of the multiplatform DA in the primary production analysis especially at the spring bloom peak. However, the result indicates that the DA system needs further tuning to make a balance between multiplatform observations.

5.4.3 NWS: Multiplatform DA changes significantly the net primary production, also outside the glider area. Since the phytoplankton biomass is more realistic with the assimilated glider chlorophyll, the natural expectation is that the net primary production is improved by the glider DA.

5.5 Phytoplankton functional types

In SEAMLESS, the **Phytoplankton Functional Types** (PFT) indicator is defined as the ratio between large phytoplankton biomass and total phytoplankton biomass. (Deliverable D3.2)

5.5.1 MED: Multiplatform DA impacts the PFT biomasses in the 3D MFC system with different patterns in different phytoplankton groups and seasons given the dynamically evolving error covariances. Changes are in the direction of improving this ecosystem indicators (based on phytoplankton biomass diagnostics in the 3D system). Additionally, large changes, up to 30%, and reduction of the ensemble spread are observed in the 1D system. Multiplatform assimilation produces changes that are not always the combination of the single observation type assimilation.

5.5.2 ARC: Multiplatform DA has only a small impact on phytoplankton community structure at some bloom peaks.

5.5.3 NWS: Multiplatform DA has only a small impact on phytoplankton community structure.

5.6 Trophic efficiency

In SEAMLESS, the **trophic efficiency** is the ratio of production at one trophic level to production at the next lower trophic level. See Table 2.1 of D2.1 for the definition for each of our BGC models. (Deliverable D3.2)

5.6.1 MED: Multiplatform DA does not change significantly the trophic efficiency in the 3D system. The addition of BGC-Argo floats assimilation has limited spatial impact, but it can be locally as important as the OC assimilation, particularly during summer.

5.6.2 ARC: Multiplatform DA has medium impact on trophic efficiency by increasing zooplankton biomass during the entire spring bloom.

5.6.3 NWS: Multiplatform DA changes significantly the trophic efficiency, also outside the glider area.

The following summary table wraps up the potential impacts when using multiplatform assimilation compared to single sensor (i.e., Ocean Color) data assimilation. When changes can be assessed in terms of skill performance diagnostics the impact is reported in terms of improvements or degradations; otherwise, the impact is reported only on a qualitative basis ("no impact" or small/medium/large "changes"). pH and O2 are not evaluated in MED and ARC given the limited controllability of chlorophyll assimilation on these variables (Deliverable 3.2). O2 is directly assimilated in the NWS domain and its impact is shown in Figure 4.3.12 and reported in table 5.1.

Indicator	MED	ARC	NWS
Phenology	N/A	Medium changes	Large changes
PP	Small changes	Medium changes	Large changes
POC flux	Small changes (moderate improvements)	N/A	Medium changes
PFT	Changes (moderate improvements)	Small changes	Small changes
Trophic efficiency	Small changes	Medium changes	Large changes
pH	N/A	N/A	Small changes
O2	N/A	N/A	Large changes

Table 5.1. impact of the multiplatform data assimilation with respect to OC-only data assimilation to the SEAMLESS ecosystem indicators.

Discussion and conclusions

There are very few examples in the scientific literature of joint biogeochemical assimilation of surface data (e.g., ocean color) and in situ data (e.g., chlorophyll, oxygen or nutrient profiles). In the context of the Copernicus Marine Service, biogeochemical Monitoring and Forecast Centers (MFCs) generally assimilate ocean color observations only. The SEAMLESS project, while proposing the joint assimilation of surface and profile observations, has several novel elements: (i) ensemble approaches for uncertainty and covariance estimation and analysis phase; (ii) a two-stage approach: first the 1D prototype for sensitivity analysis and then the 3D MFC domains for impact analysis of the existing multiplatform observing systems; (iii) some relevant ecosystem indicators (e.g.., POC sink, primary production, ...), which are used to evaluate the impact of multiplatform data assimilation.
Three Copernicus MFC domains are involved in this task (NWS, ARC and MED). The results of numerical experiments have shown that multiplatform data assimilation is important for sub-surface processes of phytoplankton dynamics, such as the onset and variability of the deep chlorophyll maximum. Multiplatform DA enhances subsurface assimilated variables (e.g., chlorophyll and oxygen) by optimally combining the capabilities of its components: in general, overall capabilities are comparable to the ones of any single component. Covariances calculated on the basis of a dynamically evolving ensemble allow information from assimilated variables to be transferred to other model components without significant degradation of non-assimilated variables (e.g., nutrients or among the PFT groups).

Thus, considering the WP5 hypotheses, our results show that the integration of the satellite observations and in situ profile data have a positive impact on the controllability of biogeochemical states and processes along the water column even if the quantification might be limited by the poor availability of independent data. Additionally, our ensemble application proved to be capable to handle consistently model covariances linking surface to subsurface processes without generating degradations in biogeochemical dynamics.

Within the list of the SEAMLESS indicators, those related to phytoplankton dynamics are the ones mostly positively impacted by the addition of profiles assimilation (i.e., larger changes and reduction in ensemble spread). It appears that primary production, POC sink, and phytoplankton functional group biomasses benefit most from the addition of in situ observations to the standard ocean color assimilation. However, the lack of independent validation datasets of the indicators remains an open issue for a conclusive claim that the changes are improvements.

Because in situ observations (e.g., glider or float profiles) are generally rare and sparse, their impacts are expected to be spatially limited to the areas around their trajectories and, during winter, the OC assimilation often overwhelms in situ assimilation. However, it is worth noting that the extent of the areas of influence is determined by the temporally evolving spatial covariances, rather than a predetermined and fixed correlation length scale as in previous systems such as variational 3DVAR (for MED and NWS). Additionally, our results show that some effects of in situ assimilation can occur well outside the observed areas. The mechanism of signal propagation outside the neighborhood of the float or glider trajectories needs further investigation.

Another important aspect of insitu profiling platforms is that they can measure additional variables other than chlorophyll (e.g. nitrate, oxygen, bbp700 as proxy of the phytoplankton biomass). These additional variables can be used for multivariate data assimilation with benefits for other biogeochemical model components as done in the NWS experiments or as shown in other assimilation frameworks (Teruzzi et al,. 2021; Wang et al., 2020). Thus, it is strongly recommended that the in situ observing systems (e.g., gliders and floats) are further supported and expanded to enhance their positive impact on the operational forecast modeling systems.

There are discrepancies between Ocean Color and in situ observations at the surface (e.g., chlorophyll from satellite and BGC-Argo or Glider). The ensemble methods handle these discrepancies without causing shocks or degradations in the simulations (e.g., in the MED and NWS). In the case of the Norwegian Sea (part of the ARC domain), no discrepancies are observed between satellite and BGC-Argo. The values of the observation error could be different between the two platforms considering the different nature of the chlorophyll retrieval processes and the representative error of the two measurements. The impact of the error difference between the two platforms on the data assimilation analysis is not yet clear and needs further investigation (All MFCs).

The 1D prototype system provides useful indications of the sensitivity of the various elements (e.g., frequency, error, and spatial resolution of the observations) of the ensemble multiplatform approach, which are useful for implementing the model setup in the 3D MFC domains.

However, in the 3D MFC systems, it may still be necessary to tune certain aspects of the setup to achieve effective assimilation, as was the case with the previously implemented non-ensemble methods. For example, the hybrid ensemble 3DVAR (NWS) and the SEIK (MED) applications are reported to be less efficient to constrain on the assimilated variables than the previous 3DVAR systems. The errors of the different observation types could be individually tuned to account for correlation effects between dense observations. Selecting different observation errors may increase the influence of sparse observations (typically in situ). In addition, tuning observational errors may also be necessary because of data quality control issues in RT for the observing system.

Finally, the computational cost of the full 3D MFC domain ensemble simulation remains an overwhelming obstacle to effective tuning of multiplatform assimilation and rapid implementation of biogeochemical ensemble approaches in the near real time operational system, but can be considered for the delayed mode reanalysis productions as in the ARC.

References

Bittig, H. C., Maurer, T. L., Plant, J. N., Schmechtig, C., Wong, A. P., Claustre, H., & Xing, X. (2019). A BGC-Argo guide: Planning, deployment, data handling and usage. Frontiers in Marine Science, 6, 502

Butenschön, M., Clark, J., Aldridge, J. N., Allen, J. I., Artioli, Y., Blackford, J., & Torres, R. (2016). ERSEM 15.06: a generic model for marine biogeochemistry and the ecosystem dynamics of the lower trophic levels. *Geoscientific Model Development*, *9*(4), 1293-1339.

Ciavatta, S., Torres, R., Martinez-Vicente, V., Smyth, T., Dall'Olmo, G., Polimene, L., & Allen, J. I. (2014). Assimilation of remotely-sensed optical properties to improve marine biogeochemistry modelling. Progress in Oceanography, 127, 74-95

Ciavatta, S., Kay, S., Saux‐Picart, S., Butenschön, M., & Allen, J. I. (2016). Decadal reanalysis of biogeochemical indicators and fluxes in the North West European shelf‐sea ecosystem. Journal of Geophysical Research: Oceans, 121(3), 1824-1845.

Ciavatta, S., Brewin, R. J. W., Skakala, J., Polimene, L., de Mora, L., Artioli, Y., & Allen, J. I. (2018). Assimilation of ocean‐color plankton functional types to improve marine ecosystem simulations. Journal of Geophysical Research: Oceans, 123(2), 834-854

Ciavatta, S., Kay, S., Brewin, R. J., Cox, R., Di Cicco, A., Nencioli, F.,Tsapakis, M. (2019). Ecoregions in the Mediterranean Sea through the reanalysis of phytoplankton functional types and carbon fluxes. Journal of Geophysical Research: Oceans, 124(10), 6737-6759

Cossarini, G., Mariotti, L., Feudale, L., Mignot, A., Salon, S., Taillandier, V., d'Ortenzio, F. (2019). Towards operational 3D-Var assimilation of chlorophyll Biogeochemical-Argo float data into a biogeochemical model of the Mediterranean Sea. Ocean Modelling, 133, 112-128

Fennel, K., Gehlen, M., Brasseur, P., Brown, C. W., Ciavatta, S., Cossarini, G Crise A, Edwards CA, Ford D, Friedrichs MAM, Gregoire M, Jones E, Kim H-C, Lamouroux J, Murtugudde R, Perruche C and GODAE OceanView Marine Ecosystem Analysis and Prediction Task Team. (2019). Advancing marine biogeochemical and ecosystem reanalyses and forecasts as tools for monitoring and managing ecosystem health. Frontiers in Marine Science, 6, 89.

Fontana, C., Brasseur, P., & Brankart, J. M. (2013). Toward a multivariate reanalysis of the North Atlantic Ocean biogeochemistry during 1998–2006 based on the assimilation of SeaWiFS chlorophyll data. Ocean Science, 9(1), 37-56.

Ford, D., & Barciela, R. (2017). Global marine biogeochemical reanalyses assimilating two different sets of merged ocean colour products. Remote Sensing of Environment, 203, 40-54.

Ford, D. (2021). Assimilating synthetic Biogeochemical-Argo and ocean colour observations into a global ocean model to inform observing system design. Biogeosciences, 18(2), 509-534.

Gehlen, M., Barciela, R., Bertino, L., Brasseur, P., Butenschön, M., Chai, F., Simon, E. (2015). Building the capacity for forecasting marine biogeochemistry and ecosystems: recent advances and future developments. Journal of Operational Oceanography, 8(sup1), s168-s187.

Goodliff, M., Bruening, T., Schwichtenberg, F., Li, X., Lindenthal, A., Lorkowski, I., & Nerger, L. (2019). Temperature assimilation into a coastal ocean-biogeochemical model: assessment of weakly and strongly coupled data assimilation. Ocean Dynamics, 69, 1217-1237

Groom, S., Sathyendranath, S., Ban, Y., Bernard, S., Brewin, R., Brotas, V., Wang, M. (2019). Satellite ocean colour: current status and future perspective. Frontiers in Marine Science, 6, 485.

Hu, J., Fennel, K., Mattern, J. P., & Wilkin, J. (2012). Data assimilation with a local Ensemble Kalman Filter applied to a three-dimensional biological model of the Middle Atlantic Bight. Journal of Marine Systems, 94, 145-156

Kaufman, D. E., Friedrichs, M. A., Hemmings, J. C., & Smith Jr, W. O. (2018). Assimilating bio-optical glider data during a phytoplankton bloom in the southern Ross Sea. Biogeosciences, 15(1), 73-90

Jones, E. M., Baird, M. E., Mongin, M., Parslow, J., Skerratt, J., Lovell, J., Taylor, J. (2016). Use of remote-sensing reflectance to constrain a data assimilating marine biogeochemical model of the Great Barrier Reef. Biogeosciences, 13(23), 6441-6469

Le Traon, P. Y., Reppucci, A., Alvarez Fanjul, E., Aouf, L., Behrens, A., Belmonte, M., ... & Zacharioudaki, A. (2019). From observation to information and users: The Copernicus Marine Service perspective. Frontiers in Marine Science, 6, 234

Liu, Y., Meier, H. E., & Eilola, K. (2017). Nutrient transports in the Baltic Sea–results from a 30-year physical–biogeochemical reanalysis. Biogeosciences, 14(8), 2113-2131.

Mattern, J. P., Song, H., Edwards, C. A., Moore, A. M., & Fiechter, J. (2017). Data assimilation of physical and chlorophyll a observations in the California Current System using two biogeochemical models. Ocean Modelling, 109, 55-71

Nerger, L., & Gregg, W. W. (2007). Assimilation of SeaWiFS data into a global ocean-biogeochemical model using a local SEIK filter. Journal of Marine Systems, 68(1-2), 237-254.

Nerger, Lars, and Watson W. Gregg. "Improving assimilation of SeaWiFS data by the application of bias correction with a local SEIK filter." Journal of marine systems 73.1-2 (2008): 87-102.

Nerger, L., Janjić, T., Schröter, J., & Hiller, W. (2012). A unification of ensemble square root Kalman filters. Monthly Weather Review, 140(7), 2335-2345.

Pradhan, H. K., Voelker, C., Losa, S. N., Bracher, A., & Nerger, L. (2019). Assimilation of global total chlorophyll OC-CCI data and its impact on individual phytoplankton fields. Journal of Geophysical Research: Oceans, 124(1), 470-490

Pradhan, H. K., Völker, C., Losa, S. N., Bracher, A., & Nerger, L. (2020). Global assimilation of ocean-color data of phytoplankton functional types: Impact of different data sets. Journal of Geophysical Research: Oceans, 125(2), e2019JC015586

Salon, S., Cossarini, G., Bolzon, G., Feudale, L., Lazzari, P., Teruzzi, A., Crise, A. (2019). Novel metrics based on Biogeochemical Argo data to improve the model uncertainty evaluation of the CMEMS Mediterranean marine ecosystem forecasts. Ocean Science, 15(4), 997-1022

Simon, E., Samuelsen, A., Bertino, L., & Mouysset, S. (2015). Experiences in multiyear combined state–parameter estimation with an ecosystem model of the North Atlantic and Arctic Oceans using the Ensemble Kalman Filter. Journal of Marine Systems, 152, 1-17

Shulman, I., Frolov, S., Anderson, S., Penta, B., Gould, R., Sakalaukus, P., & Ladner, S. (2013). Impact of bio-optical data assimilation on short-term coupled physical, bio-optical model predictions. Journal of Geophysical Research: Oceans, 118(4), 2215-2230

Sathyendranath, S.; Jackson, T.; Brockmann, C.; Brotas, V.; Calton, B.; Chuprin, A.; Clements, O.; Cipollini, P.; Danne, O.; Dingle, J.; Donlon, C.; Grant, M.; Groom, S.; Krasemann, H.; Lavender, S.;

Mazeran, C.; Mélin, F.; Moore, T.S.; Müller, D.; Regner, P.; Steinmetz, F.; Steele, C.; Swinton, J.; Valente, A.; Zühlke, M.; Feldman, G.; Franz, B.; Frouin, R.; Werdell, J.; Platt, T. (2020): ESA Ocean Colour Climate Change Initiative (Ocean_Colour_cci): Global chlorophyll-a data products gridded on a sinusoidal projection, Version 4.2. Centre for Environmental Data Analysis, date of citation. https://catalogue.ceda.ac.uk/uuid/99348189bd33459cbd597a58c30d8d10.

Skákala, J., Ford, D., Brewin, R. J., McEwan, R., Kay, S., Taylor, B., ... & Ciavatta, S. (2018). The assimilation of phytoplankton functional types for operational forecasting in the northwest European shelf. Journal of Geophysical Research: Oceans, 123(8), 5230-5247

Skakala, J., Bruggeman, J., Brewin, R. J., Ford, D. A., & Ciavatta, S. (2020). Improved representation of underwater light field and its impact on ecosystem dynamics: A study in the North Sea. *Journal of Geophysical Research: Oceans*, *125*(7), e2020JC016122.

Skakala, J., Ford, D., Bruggeman, J., Hull, T., Kaiser, J., King, R. R., ... & Ciavatta, S. (2021). Towards a multi-platform assimilative system for North Sea biogeochemistry. Journal of Geophysical Research: Oceans, 126(4), e2020JC016649

Teruzzi, A., Bolzon, G., Feudale, L., & Cossarini, G. (2021). Deep chlorophyll maximum and nutricline in the Mediterranean Sea: emerging properties from a multi-platform assimilated biogeochemical model experiment. Biogeosciences, 18(23), 6147-6166

Teruzzi, A., Bolzon, G., Salon, S., Lazzari, P., Solidoro, C., & Cossarini, G. (2018). Assimilation of coastal and open sea biogeochemical data to improve phytoplankton simulation in the Mediterranean Sea. Ocean Modelling, 132, 46-60

Testor, P., De Young, B., Rudnick, D. L., Glenn, S., Hayes, D., Lee, C. M., ... & Wilson, D. (2019). OceanGliders: a component of the integrated GOOS. Frontiers in Marine Science, 6, 422

Tsiaras, K. P., Hoteit, I., Kalaroni, S., Petihakis, G., & Triantafyllou, G. (2017). A hybrid ensemble-OI Kalman filter for efficient data assimilation into a 3-D biogeochemical model of the Mediterranean. Ocean Dynamics, 67, 673-690

Verdy, A., & Mazloff, M. R. (2017). A data assimilating model for estimating S outhern O cean biogeochemistry. Journal of Geophysical Research: Oceans, 122(9), 6968-6988

Yu, L., Fennel, K., Bertino, L., El Gharamti, M., & Thompson, K. R. (2018). Insights on multivariate updates of physical and biogeochemical ocean variables using an Ensemble Kalman Filter and an idealized model of upwelling. Ocean Modelling, 126, 13-28.

Xiao, Y., & Friedrichs, M. A. (2014). The assimilation of satellite-derived data into a one-dimensional lower trophic level marine ecosystem model. Journal of Geophysical Research: Oceans, 119(4), 2691-2712

Wang, B., Fennel, K., Yu, L., and Gordon, C.: Assessing the value of biogeochemical Argo profiles versus ocean color observations for biogeochemical model optimization in the Gulf of Mexico, Biogeosciences, 17, 4059–4074, https://doi.org/10.5194/bg-17-4059-2020, 2020

Widdicombe, C. E., Eloire, D., Harbour, D., Harris, R. P., & Somerfield, P. J. (2010). Long-term phytoplankton community dynamics in the Western English Channel. Journal of plankton research, 32(5), 643-655